ANALYSIS OF FATTY ACID METABOLISM-RELATED GENE EXPRESSION IN DIABETIC RAT HEARTS

By

Jin Wu
Bachelor of Sciences
Yantai University 1990

THESIS SUBMITTED IN PARTIAL FULFILLMENT OF
THE REQUIREMENTS FOR THE DEGREE OF

MASTER OF SCIENCES

In the
Department
of
Biological Science

SIMON FRASER UNIVERSITY

Fall 2005

APPROVAL

Name: **Jin Wu**

Degree: **Master of Science**

Title of thesis **ANALYSIS OF FATTY ACID METABOLISM-RELATED GENE EXPRESSION IN DIABETIC RAT HEARTS**

Examining Committee:

Chair **Dr. Eirikur Palsson** Assistant Professor

Dr. Norbert Haunerland
Senior Supervisor

Professor of Biological Sciences,

Simon Fraser University

Dr. Margo Moore
Supervisor

Professor of Biological Sciences,

Simon Fraser University

Dr. Aine L. Plant
Supervisor

Associate Professor of Biological Sciences,

Simon Fraser University

Dr. Jim Mattsson
Examiner

Assistant Professor of Biological Sciences,

Simon Fraser University

Date Defended/Approved: Sept. 23/2005

ABSTRACT

The morbidity and mortality of Diabetes mellitus is in part due to its vascular complications. Therefore, it is important to identify cellular and molecular mechanisms of vascular damage early in the diabetic state. The purpose of this thesis research was to develop techniques to identify genes that are differentially expressed in the hearts of control and diabetic rats, using macroarray and real-time PCR techniques. The array experiments identified numerous genes with altered mRNA levels, including several genes involved in lipid and carbohydrate metabolism, and ion channelling. For selected genes, the expression changes were verified by real-time PCR. Generally, the direction of gene expression changes was similar between macroarray and real-time PCR experiments, but the numerical changes significantly differed between the two methods. Thus, macroarray analysis is a valid survey technique to identify potential gene expression changes in the heart of diabetic rats, but quantitative analysis requires verification by real-time PCR.

DEDICATION

To my family and my lovely son Paul for their everlasting love and support.

ACKNOWLEDGEMENTS

I express my sincerest thanks to Dr. N. Haunerland, my senior supervisor, and my supervisor Dr. Jutta Huanerland, for their patient guidance and encouragement throughout my whole project, for their great help in improving my writing. I deeply appreciate the freedom they gave me during my graduate studies. I have learnt a lot in many ways under their supervision over the past four years.

Many thanks go to Dr. Moore and Dr. Plant, my committee supervisors, for their great help, assistance and invaluable advice.

I wish to express my genuine appreciation to Dr. Carl Lowenberger for his technical support, let me use his new and expensive Q-PCR equipment.

I also wish to thanks my labmates, Linda Chen and David Qu, for their kindly friendship and always support.

Special thanks to my family, my parents and all my friends for their everlasting love.

TABLE OF CONTENTS

LIST OF FIGURES

LIST OF TABLES

GLOSSARY

ACBP	Acyl-CoA binding protein
ACS	Acyl-CoA synthetase
CPT	Carnitine palmitoyl transferase
Ct	Threshold cycle
△CP	Crossing point deviation (control - sample)
FA	Fatty acid
FABP	Fatty acid binding protein
FACO	Fatty Acyl-CoA oxidase
FAT/CD36	Fatty acid translocase
FATP	Fatty acid transport protein
FFA	Free fatty acid
GAPDH	Glyceraldehyde-3-phosphate dehydrogenase
GLUT	Glucose transporter
LCAD	Long-chain Acyl-Coenzyme A dehydrogenase
LCM	Laser capture microdissection
LPL	Lipoprotein lipases
IDDM	Insulin-dependent diabetes mellitus
MCAD	Medium chain Acyl-CoA dehydrogenase
NIDDM	Non-insulin-dependent diabetes mellitus
NTC	No template control
PKC	Protein kinase C
qRT-PCR	Quantitative-reverse transcription polymerase chain reaction

REST	The Relative Expression Software Tool
S29	S29 fragment of ribosomal RNA
SG	SYBR Green I
SERCA	Sarcoplasmic reticulum Ca^{2+} ATPase
STZ	Streptozotocin
TGF-β	Transforming growth factor – β
VEGF	Vascular endothelial growth factor
VLDL	Very low-density lipoproteins
VLCAD	Very long chain Acyl-CoA dehydrogenase

CHAPTER 1: GENERAL INTRODUCTION

Diabetes is a disease in which the body is unable to regulate blood sugar levels. Diabetic patients are very thirsty and produce abnormally large amounts of urine, with a sweet-smelling, honey-like odour. The ancient physician could make a diagnosis by the smell of the urine, with sweet urine indicating the patient had diabetes mellitus (www.diabetesmanager.com - history). Normally, the hormone insulin regulates blood sugar levels by stimulating the uptake of glucose into the target tissues for subsequent metabolism. However, diabetes patients accumulate abnormally high levels of glucose in the blood. In diabetes, insulin is no longer capable of regulating these processes. Insulin is produced by the pancreas, which secretes two additional hormones involved in glucose homeostasis: glucagon and somatostatin. Each hormone is produced by an individual cell type; insulin is secreted from β-cells. Insulin is a small peptide with a molecule weight of 6000 Daltons, consisting of an A-chain of 21 amino acids and a B-chain of 30 amino acid residues (Steiner, 1977). Insulin is secreted from the pancreas into the bloodstream as a direct response to hyperglycemia. In addition, it is continuously released in varying rates to regulate the concentration of plasma glucose by causing some cell types to increase glucose uptake. Insulin concentration in the blood runs parallel with that of glucose, and administration of insulin promptly induces hypoglycemia.

Diabetes mellitus is classified in two types: insulin-dependent diabetes mellitus (IDDM, or type I diabetes) and non-insulin-dependent diabetes mellitus (NIDDM, or type II diabetes). Patients with IDDM are dependent on insulin injections to avoid ketosis and to sustain life. NIDDM patients generally do not require insulin injections, because the pancreas still secretes insulin, but the insulin receptor has partially lost its function (Handberg et al., 1993). This receptor, which is located in the cell membrane of target tissues, binds to insulin to initiate intracellular signalling that leads to glucose uptake (White and Kahn, 1994). In a normal, fasting human, plasma insulin concentration is 5-20 μU/ml (1 U defined as 6 nanomoles or 35 μg of insulin). However, in a diabetic patient, plasma insulin concentration may be as high as 250 μU/ml (Ling, 1996).

Diabetes mellitus is a leading cause of morbidity and mortality because diabetic patients tend to develop significant vascular problems. Several studies have shown that the mortality of diabetic patients due to cardiovascular disease is two to four times greater than in non-diabetics (Kuller et al., 2000). Diabetes and cardiovascular disease together account for the largest portion of health care spending compared to all other diseases in North America. The cost continues to increase because of the parallel trends of an aging population and an increasing incidence of obesity. From the American Diabetes Association 2002 reports, there are about 143 million patients with diabetes, which is almost 5 times more than estimated 10 years ago (American Diabetes Association, 2002). From a Canadian Diabetes Association 2003 report, there are over 2 million patients with

diabetes in Canada (Canadian Diabetes Association, 2003). Together, several billion dollars are spent annually on diabetic patients. It is therefore important to research the pathogenesis, prevention, and treatment of diabetes. Until diabetes can be prevented, clarifying the critical cellular and molecular mechanisms of vascular complications of diabetes is necessary to understand and limit the damage caused by this disease.

Many studies have shown that both metabolic and hormonal imbalances contribute to the pathogenesis of diabetic vascular diseases (Marrero and Stem, 2004). Although the underlying defect may be straightforward (i.e., lack of insulin production by the pancreatic β cells), diabetes is a complex disorder of metabolism, which includes disorder in the metabolism of carbohydrates, protein, and fats.

With regard to carbohydrate metabolism, absence of insulin or ineffective insulin activity prevents the uptake of glucose by tissues such as muscle, adipose tissue and liver. As the blood glucose level approaches 180 mg/dL, the ability of the kidney to reabsorb glucose is surpassed, and glucose is excreted into the urine. Because it is an osmotic diuretic, glucose causes the osmosis of large amounts of water into the tubules, causing frequent urination in large quantities (polyuria). Thus, clinical abnormalities include polyuria, excessive thirsty (polydipsia), and excessive eating (polyphagia).

Protein metabolism is also affected, as the body breaks down protein stores to overcome the lack of glucose, leading to a negative nitrogen balance. Protein metabolic defect leads to loss of muscle mass and weakness. Fat stores are mobilized into free fatty acids (FFAs). In the liver excess amounts of fatty acids cannot enter into the Krebs cycle and instead condense into acetoacetic acid, called ketone bodies, which cause hyperventilation, metabolic acidosis, abdominal pain.

Normally, cellular levels of glucose and fatty acid metabolism are related. Insulin indirectly suppresses lipolysis, and consequently decreases the circulating free fatty acid (FFA) concentration (McGarry and Dobbins, 1999). In diabetes, because of reduced insulin activity, the processes of glucose entering into the cell and cellular carbohydrate metabolism are impaired; glucose-processing reactions are lower than normal in the muscle cell, and consequently energy requirements are met by the oxidation of free fatty acids (Garvey et al., 1991). These metabolic abnormalities cause glucose overproduction, the inadequate disposal of ingested glucose, the dissolution of fat stores and an increase in plasma lipid levels (Goldberg, 2001). Thus, both hyperglycemia and hyperlipidemia are primarily syndromes of diabetes.

Secondary consequences of diabetes mellitus include serious systemic complications. These complications can be broadly classified into two types: microvascular and macrovascular complications (Diabetes control and

complications trial research group, 1993). Microvascular complications include retinopathy (Kahn and Hiller, 1974) and nephropathy (Breyer, 1998), while macrovascular complications include coronary artery disease, cerebrovascular disease and peripheral vascular disease (Diabetes control and complications trial research group, 1993). The impact of both IDDM and NIDDM on the macrovasculature results from accelerated atherosclerosis and increased thrombosis, and the vessels that are affected are mainly the coronary, cerebral, and peripheral arteries. The most abundant and mortal vascular disease is atherosclerotic cardiovascular disease (Bierman, 1992), which is a common cause of death among people with diabetes (Bell, 1995). Hyperglycemia, hyperlipidemia, hyperinsulinemia and decreased insulin sensitivity all contribute to the development of diabetic vascular disease.

Early studies on substrate metabolism of the human heart have revealed that, as expected, cardiac glucose uptake is decreased, whereas fatty acid (FA) uptake is increased in diabetic patients (Garvey et al., 1991). Under normal physiological conditions, 60–90 % of the metabolic energy is generated by FA mitochondrial oxidation (Brinkman et al., 2002). Myocardial ATP production under aerobic conditions arises from the mitochondrial oxidation of acetyl-CoA, derived from carbohydrates or free fatty acids. However, in the diabetic heart, fatty acid oxidation provides almost all of the energy for myocardial ATP production since glucose oxidation is essentially abolished. Normally, glucose entry into the primary insulin target tissue - skeletal muscle, heart, adipose tissue and liver - is

mediated by glucose transport protein (GLUT). GLUT4 is present in adipose tissue and cardiac, skeletal muscle and distributed mainly in a specific population of intracellular vesicles. Many studies show that insulin-stimulated GLUT4 translocation is indeed impaired in diabetic muscle (Ryder et al., 2000). The shift towards greater fatty acid oxidation is caused in part by the decrease in the number and activity of glucose transporters in the plasma membrane (Garvey et al., 1991). However, another major reason for the decrease in myocardial glucose metabolism is the elevated level of plasma fatty acids. High circulating levels of fatty acids lead to increased fatty acid sequestration, which in turn decreases glucose metabolism. These and other, less well characterized metabolic changes in the heart are also responsible for the observed low glucose oxidation rates. The reduced availability of metabolic fuels leads to reduced levels of ATP, which is an important regulator of ion channels. Thus, diabetes mellitus is a widespread and complex disorder of metabolism, including glucose, and lipid metabolism, as well as the active transport of ion. These pathways are described in more detail below.

Glucose metabolism:

In cardiomyocytes, glucose is metabolized predominantly through glycolysis to form pyruvate. Pyruvate is either converted to acetyl-CoA (oxidative metabolism) or is converted anaerobically to lactate and released from the heart. Glucose is not only an energy source for the heart, but it has multiple other functions. When

glucose is transported into cardiomyocytes, it becomes phosphorylated by hexokinase to generate glucose 6-phosphate (Fig. 1-1).

Hyperglycemia plays an important, but as yet not clearly defined role in clinical macrovascular disease. In an insulin dependent manner, cardiomyocytes take up glucose by glucose transporters (GLUT). Protein kinase C (PKC) activation is associated with insulin stimulation of glucose transport and GLUT4 translocation (Valverde et al., 2000), which implicates PKC as an important element in insulin signalling. However, the detail mechanism of PKC regulation is still not very clear. While limited clinical studies have suggested that intensive glycemia control can reduce cardiovascular disease, the actual effect of hyperglycemia on the development and progression of macrovascular complications remains unclear and even somewhat controversial. The complicated nature of the metabolic abnormalities in diabetes and the relative roles of the various associated conditions in the development of macrovascular disease make definitive conclusions somewhat difficult. At the molecular level, the expression of several genes is reported to be changed in diabetic mellitus. In cardiac tissue, mRNA levels were down-regulated for GLUT4 (67 %, Garvey et al., 1993, Hidaka et al., 1999) and hexokinase 2 (59 %, Yechoor et al., 2002). Changes in protein kinase C (PKC) expression are disputed now; one paper reports its down-regulation (51%, Yechoor et al., 2002) while another shows up-regulation (Giles et al., 1998).

Lipid metabolism:

Lipids serve many functions, including energy storage and constitution of structural elements. The major lipid classes in animals include steroids, triacylglycerols, phospholipids and their metabolic products free fatty acids (FFAs), glycerol, as well as ketone bodies. Energy is stored in the long reduced hydrocarbon chain of fatty acids and is released by oxidation. Fatty acid oxidation results in a high yield of energy, which provides most of the heat for the maintenance of body temperature, and the ATP requirement for the contraction of the heart. Compared with other food sources, the caloric value of triacylglycerols is higher per mass: lipid oxidation yields 39 kJ/g, carbohydrates 17 kJ/g and protein 17 kJ/g (Faust, 1980). Part of the dietary carbohydrate is converted to fat before it is utilized to provide energy. Cholesterol is a component of cell membranes and is the basic molecule used for steroid hormone synthesis. Lipid is transported in lipoproteins in the bloodstream. Since the serum presents an aqueous environment, more hydrophobic, less soluble lipids combine with polar molecules such as phospholipids and proteins to form lipoproteins. They are assembled in the intestine or liver and released into the blood as chylomicrons and very low-density lipoproteins (VLDL) (Eisenberg et al., 1976). Lipoprotein-bound FFA is hydrolyzed at the target tissues (e.g., heart muscle) to free fatty acids and glycerol by lipoprotein lipases (LPL). Free fatty acid is taken up by various tissues and oxidized in the mitochondrial matrix. The uptake process into cells is still controversial. It may occur partly by diffusion, but seems

to involve also various transport proteins, including fatty acid translocase (CD36), fatty acid transport proteins (FATP), or plasma membrane fatty acid binding protein ($FABP_{PM}$)(Chiu et al., 2001). Within the cell, cytosolic fatty acid binding proteins carry the fatty acids through the cytosol (Haunerland, 1994). Finally, fatty acids are converted to their acyl-CoA esters by acyl-CoA synthetases, and shuttled into mitochondria, where β-oxidation takes place (Figure1-1).

The major portion of normal lipid synthesis and metabolism is directed toward internal use of these components required by various organs and tissues. There are, however, several disease conditions, where lipid synthesis and metabolism are impaired, leading to alteration of the membrane structure and subsequent abnormal function or to an accumulation of lipids in various tissues. High fatty acid in serum and tissue triglycerides and cholesterol are associated with atherosclerosis (Steiner, 2000). Clinical studies show that diabetic patients have more atherosclerosis and a higher risk of developing coronary heart disease (CHD) (Haffner et al., 1990).

Diabetes leads to disorders of fatty acid metabolism. Normally the levels of intracellular fatty acids and their derivatives are tightly regulated. To respond to elevations in fatty acid levels, mammalian organisms increase the expression of various proteins involved in fatty acid utilization. The mechanism by which elevated fatty acid levels activate the transcription of these genes is still not very clear. The synthesis of the following proteins has been reported to be up-

regulated in diabetic hearts: FABP (134–191 % of normal levels, Glatz, 1994, Hidaka et al., 1999, Engels et al., 1999), fatty acyl-CoA oxidase (FACO, 265 %, Engels et al.,1999), acyl-CoA synthetase (ACS), long-chain acyl-CoA dehydrogenase (LCAD) (Andries et al., 2003), medium chain acyl-CoA dehydrogenase (MCAD, 138 %), carnitine acetyltransferase (165 %), acyl-CoA thioesterase 1 (371 %), fatty acid transporter 1 (FAT/CD36) (2818 %) (Yechoor et al., 2002). Down-regulation was demonstrated for creatine kinase (84 %, Yechoor et al., 2002).

Ion channel system:

Metabolism of glucose is closely related to the ratio of ATP to ADP, while ATP interacts with ATP-dependent ion channels (Newgard and McGarry, 1995). In diabetes, abnormal glucose metabolism affects ion-channel related enzyme activity. Clinical studies have shown that heart muscle from diabetic animals exhibits a slow rate of relaxation (Sowers et al., 2001). It has also been shown that abnormalities of intracellular Ca^{2+} flow cause cardiac dysfunction in streptozotocin (STZ) induced diabetic rats, which is a rat model for insulin-dependent diabetic. Therefore, the regulation of the plasma membrane sodium calcium exchanger is considered an important factor in the pathology of diabetes. In addition, it is reported that Sarcoplasmic reticulum Ca^{2+} ATPase (SERCA) 2 activity decreases in response to pressure overload and diabetes (Pierce et al., 1988). Reduction in SERCA activity has been considered a major cause of contractile dysfunction. It has been demonstrated that the metabolic status of the

cardiomyocyte influences the transcription rates of SERCA2a. Defects in the sarcolemmal Ca^{2+} pump and Na^{+}-Ca^{2+} exchanger, decreased Ca^{2+} current and dysfunction of the sarcoplasmic reticulum (SR) were emerging in the STZ diabetic heart. In addition, insulin-deficient type I diabetes is associated with early down-regulation of the expression of key cardiac K^{+} channel genes that could account for the depression of cardiac K^{+} currents in diabetic heart. These represent the main electrophysiological abnormalities associated with diabetic cardiomyopathy. Thus, to investigate changes in the regulation of ion channel in the diabetic heart is important for improving diagnostic and therapeutic strategies. Gene expression changes for ion channel genes reported include sarcoplasmic reticulum Ca^{2+}-ATPase (SERCA 2a, down regulated, Young et al., 2002, Vetter et al., 2002, Teshima et al., 2000), and Na/K-ATPase (down regulated, Golfman et al., 1998). In addition to the depressed calcium ion transport, Na^{+}-H^{+} and Na^{+}-Ca^{2+} exchange are also depressed (Pierce et al., 1990).

In addition to genes involved in glucose, lipid, and ion homeostasis, many other genes are also differentially expressed in diabetic animals. Diabetes is associated with increased expression and action of various cytokines and growth factors. For example, vascular endothelial growth factor (VEGF) is produced by retinal cells in response to hypoxia (Pierce et al., 1995). It is a potent mediator of vascular permeability and vascular endothelial proliferation (Plate, 1992). VEGF has been considered to play a pivotal role in mediating proliferative diabetic retinopathy. Transforming growth factor–β (TGF-β) has been implicated in

mediating the accumulation of extracellular matrix in the kidney and nephropathy (Choi et al., 1996, Lee et al., 2000). However, its role in diabetes is not well characterized. Thus, cytokines play a role in various diabetes-induced injuries, and it is assumed that changes in their regulation also affect the pathology of diabetes.

As outlined above, the expression of numerous genes is altered in the diabetic state. To date, only some select genes have been studied, but given the complex metabolic changes that occur as a consequence of diabetes, many more are expected to be affected either directly or indirectly. One mechanism that is of particular interest to our laboratory is the regulation of gene expression by the increased intracellular fatty acid levels that are observed in diabetes.

Comparative analysis of gene expression in experimentally-induced diabetes and in cultured cells exposed to increased fatty acid levels may allow us to separate gene regulatory mechanisms causing from increased fatty acids from others that are glucose, ion, or hormone dependent. As a first step towards this analysis, a survey of gene expression changes in experimentally-induced diabetes was necessary. Several animal models have been employed as diabetic models. Such models system involve the surgical removal of all or a large portion of the pancreas, or chemical destruction of the islets of Langerhans (the site of β cells) using agents such alloxan, dehydroascorbic acid, dithizone, or streptozotocin (STZ). These chemicals produce a selective necrosis of the β-cells. Alternative

models employ inactivatation of the circulating insulin by the administration of the antibodies against its own insulin (McNeill, 1999). We choose STZ-induced diabetic rats to study gene expression changes because it is currently the most commonly-used animal model. Streptozotocin is a compound whose chemical structure is similar to that of glucose, and upon injection, STZ destroys the pancreatic β-cells. Once depleted of pancreatic β-cells, the rats develop hyperglycemia within a few weeks. In the STZ model, a decrease in cardiac function usually appears after 6-8 weeks (Afzal et al., 1988). After that time, the levels of glucose, cholesterol, and triacylglycerols remain increased in STZ-diabetic rats (Ziegelhoffer-Mihalovicova et al., 2003). Therefore, we studied tissue from rats 12 weeks after STZ treatment, which should display the characteristic cardiovascular pathology of diabetes.

The purpose of this thesis research was to identify genes that are differentially expressed in the hearts of STZ-induced diabetic animals. Due to our interest in fatty acid mediated gene regulation, particular emphasis was placed on genes related to energy metabolism. While microarray technology could be used for such studies, the high costs make this technique unsuitable for the multiple experiments required in our studies. A more affordable alternative way is the membrane-based macroarray for studying changes in gene expression patterns, followed by real time PCR experiments to evaluate the validity of the macroarray results.

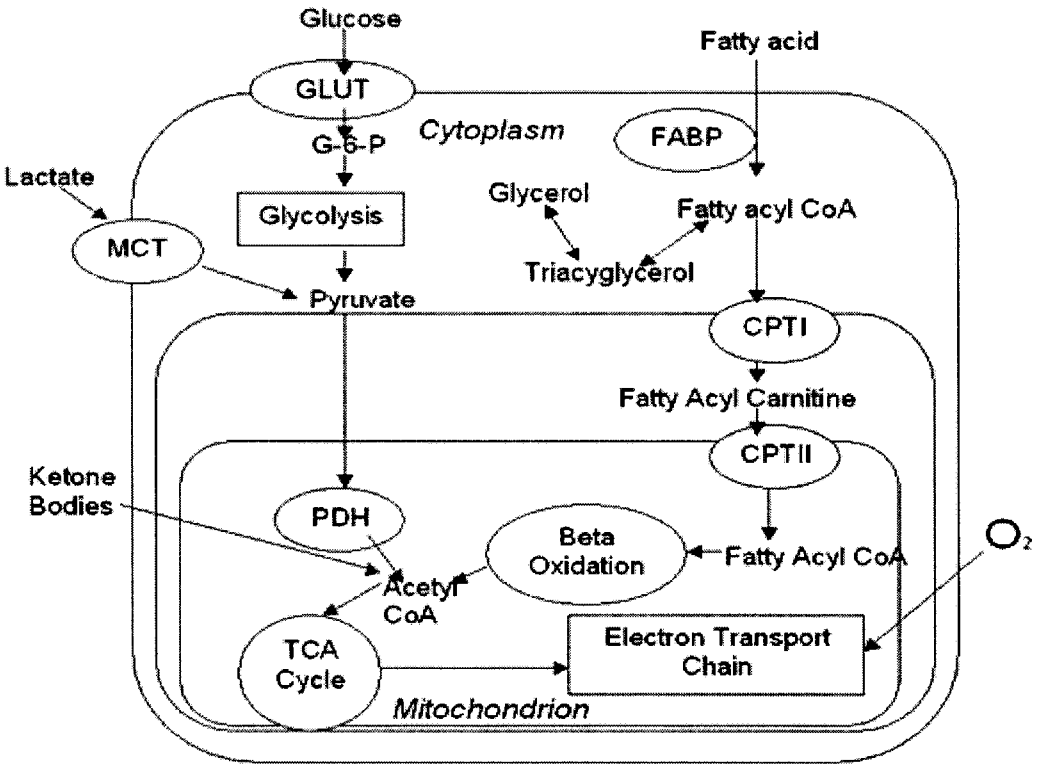

Fig. 1-1: Energy metabolism in diabetic heart muscle cells.

G-6-P = Glucose-6-phosphate; CPT = carnitine palmitoyl transferase;
GLUT = glucose transporter. FABP = fatty acid binding protein
PDH = phosphate dehydrogenase MCT = monocarboxylate transporters

CHAPTER 2: OPTIMIZATION OF THE MACROARRAY TECHNIQUE

2.1 Introduction

Traditional methods for the quantification of gene expression, such as RT-PCR, RNase protection assays, or Northern blot analysis, only focus on single genes at a time. Therefore, these techniques are not suitable to determine global gene expression changes in the diabetic heart. Approximately 10 years ago, microarray techniques were developed that can rapidly analyze gene expression changes for many genes in one experiment. Most microarrays used now are DNA arrays, which hybridize with mRNA or cDNA. In addition, there are also protein or oligonucleotide microarrays. DNA Microarrays can have as many as 500,000 specifically defined gene spots on a 1.25 cm^2 glass slide. The very small size of the spots and their high density necessitate the use of sophisticated instruments for the accurate measurements of bound DNA. Therefore, macroarrays have been developed to reduce the technological challenges, and to make array analysis more affordable (Weimer et al., 2004, Xie, 2003). In macroarrays, fewer genes (~1000) are spotted on nylon membranes (~10x18cm), with larger spots located further apart.

Both macro- and microarrays are useful to simultaneously study the expression of many genes, and to compare their expression levels in different samples. For example, alterations in the gene expression between normal and pathological samples can be measured or differential gene expression occurring during growth or as the result of environmental influences, such as the infection of human monocytes with *Staphylococcus aureus* (Wang et al., 2000, Rosenberger et al., 2001).

In the research presented in this chapter, I determined gene expression changes in the rat heart in experimental diabetes, by comparing expression levels in control rats and STZ-induced diabetic animals. Of particular interest were genes that are involved in energy metabolism. After considering the expense and technical challenges of micro- and macroarrays, we decided to use DNA macroarrays. We chose a commercially-available macroarray, the Atlas Rat 1.2 (Clontech, Mississauga, ON). These contain 1176 spots of well-characterized cDNAs, located on 4'X 7' nylon membranes, which includes many genes involved in lipid metabolism, energy metabolism, carbohydrate metabolism, as well as many ATPase transporters and voltage-gated ion channels. Most importantly, they also contain fatty acid metabolism-related genes, including various fatty acid binding proteins (FABP), mitochondrial carnitine O-palmitoyltransferase (CPT), and various acyl-CoA dehydrogenases (The gene list is available on http://www.clontech.com/clontech/atlas/genelists/index.shtml

website). My project focused especially on studying these fatty acid metabolism related genes.

Prior to any analytical work, the experimental conditions for this array analysis had to be optimized. Moreover, since array membranes are quite expensive, it was desirable to re-use these membranes several times. Part of my task was to find a gentle stripping method which left the DNA on the membrane intact, but removed completely the bound probes. Thus, our initial experiments focused on producing degradable probes that could be cleaved into smaller fragments and thus removed at milder conditions (Ambion Strip-EZ^{TM} RT kit).

2.2 Methods and Materials

2.2.1 Material

Rat skeletal muscle cells (L6 cell) were purchased from ATCC (American Type Culture Collection, Rockville, MD). Dulbecco's modified eagle's medium (DMEM), fetal bovine serum (FBS) and trypsin were obtained from GIBCO BRL (Burlington, ON), penicillin, streptomycin and bovine serum albumin (BSA) from Sigma, (Oakville ON) . The Trizol reagent came from Invitrogen (Rockville, MD), and the RNeasy Kits from Qiagen (Valencia, CA).

Atlas™ Rat 1.2 cDNA Expression Arrays, the Atlas™ SpotLight™ Labelling Kit and the SpotLight Chemiluminescent Hybridization & Detection kit were obtained from Clontech (Mississauga, ON). Alternative probe preparation was accomplished with the Strip-EZ™ RT kit (Ambion, Austin, Texas). For RNA isolation, Qiagen RNeasy Midi Kits (Qiagen, USA) were used.

2.2.1.1 Cell Culture

L6 myoblast cells (American Type Culture Collection, Rockville, MD) were cultured in DMEM supplemented with 10 % fetal bovine serum and 2 % penicillin and streptomycin solution. When confluence was reached, cells were washed with PBS-versene buffer, detached with 2.5 % trypsin, and then diluted and sub-cultured in the fresh DMEM medium.

2.2.1.2 Rat heart tissue

Animal handling and induction of diabetes was performed by Lily Chen of the Faculty of Pharmaceutical Sciences, University of British Columbia (UBC). Male Wistar rats, weighing 190–220 g, were obtained from Charles River Laboratories (Montreal, PQ). The animals were housed at UBC, in accordance with the principles and guidelines of the Canadian Council on Animal Care. Rats were

housed individually in the treated groups and in pairs in the control groups, on a 12-h light, 12-h dark schedule, and given food and fluid ad libitum. Animals were monitored for their health during the first week after arrival and then were randomly assigned to two groups: control and diabetic. Experimental diabetes was induced in rats by a single intravenous injection of streptozotocin dissolved in 0.9% saline (60 mg/kg, iv) under halothane anesthesia. Control rats were injected with 0.9% saline. Three days post STZ injection, rats with blood glucose levels higher than 14 mM were considered diabetic. After 12 weeks, rats were anesthetized with pentobarbital (65 mg/kg, ip) and killed.

Hearts were removed immediately, rinsed with sterile PBS and stored in RNAlater (Ambion, Austin, Texas) for up to 4 h, then frozen quickly in liquid nitrogen and stored at -80 °C until RNA isolation.

2.2.2 Methods

2.2.2.1 RNA extraction

Cells contain three types of RNA: messenger RNA (mRNA), transfer RNA (tRNA) and ribosomal RNA (rRNA). Ribosomal RNA constitutes more than 75% of the total RNA. Eukaryotic ribosome's separate into 28S, 18S and 5S subunits, while in prokaryotic cells, 23S, 16S and 5S subunits are found (Van Holde and Hill, 1974). tRNA is small RNA molecule, containing 72 to 95 nucleotides. tRNA

recognizes the codons on the mRNA and transfers the corresponding amino acids to the newly synthesized protein chain. Finally, mRNAs are a single strand copy of the coding region of DNA and are the template for the translation of proteins. While thousands of proteins are expressed in each cell, the mRNA molecules combined constitute normally 5 % or less of the total RNA. Because mRNA is an exact copy of the DNA coding regions, which contains genetic information, mRNA analysis can be used to identify polymorphisms in coding regions of DNA; more importantly, quantitative analysis of mRNA levels can be used as a measure of gene expression.

RNA analysis provides information both on the genetic potential of an organism and the dynamic changes at different times or functional states. Transcription rates and transcript concentrations vary widely because of different rates of transcription, and differences in RNA stability. An mRNA can be transcribed at rates of up to several hundred nucleotides per minute; however, it occurs often at much slower rates. From initiation of transcription to its ultimate degradation, the lifespan of an mRNA molecule is complex (Kim et al., 2003). This procedure is influenced by the rate of transcription, the stability of the mRNA molecule, and is also changed by internally or externally initiated cellular events. Thus, gene expression measurements quantify the concentration of each mRNA as a snapshot at a single time point. RNA concentration is normally expressed not in absolute values, but relative to another mRNA species.

RNA is unstable and is easily degraded. In biological samples, RNA molecules are even less stable, due to the presence of abundant endo- and exonucleolytic ribonucleases (RNases) (Condo and Putzer, 2002). Therefore, it is a challenge to isolate RNA from tissue and cultured cells rich in RNases. During cell disruption, RNases must be inactivated. Chaotropic agents, such as guanidinium isothiocyanate, EDTA and other compounds, are used to inhibit RNases.

Isolation of intact RNA, especially mRNA, is especially critical for quantitative experiments like qRT-PCR, real time PCR and gene arrays. For these studies, it is equally critical to quantitatively convert mRNA into complementary DNA. The quality of the RNA used for the production of micro- and macroarray probes, and for real time RT-PCR, is the most important factor for sensitivity and reproducibility. A poor RNA preparation leads to high background and inaccurate data. Thus, it was necessary to optimize the procedure for the isolation of RNA for the subsequent quantitative experiments. This optimization and the evaluation of RNA quality and integrity are described in this section.

2.2.2.2 Total RNA extraction from cultured L6 cell

Total RNA was extracted from ~$2x10^7$ cultured L6 cells using the Qiagen RNeasy Midi kit. The harvested cell pellet was washed with PBS, 4 ml RLT buffer of the Qiagen RNeasy Kit were added, and the mixture was homogenized by 10 strokes with an RNase-free 1 ml syringe, fitted with a 20 gauge needle. About 4

ml of 70 % ethanol was added to the resulting lysate, mixed well and then transferred to an RNeasy column and spun for 1 min at 12000 x g. The column was then washed once with 4 ml of buffer RW1, and twice with 2.5 ml of buffer RPE. Finally, RNA was eluted by two washes with 150 µl DEPC water each. Sodium acetate (6 µl of a 3 M solution, pH 5.2) and ethanol (1 ml) was added, and after 15 min the mixture was centrifuged for 15 min at 12000 x g, 4 °C. The RNA pellet was washed with 500 µl of 75 % ethanol twice. Following evaporation of the solvent (30 min in the fume hood), the RNA pellet was re-suspended in 20 µl DEPC-treated water.

2.2.2.3 Small scale extraction of total RNA from rat heart tissue

Total cellular RNA was extracted from rat heart tissues using Trizol reagent and the Qiagen RNeasy mini kit together. RNA was extracted from about 10 mg rat heart tissue (part of ventricle), which was homogenized in 1 ml ice-cold Trizol reagent. The homogenate was passed through the syringe 10 times to homogenize it completely, and incubated 5 min at 4 °C. Chloroform (2/10 of the volume of the homogenate) was added and the tube inverted and kept on ice for 3 min. The sample was spun for 10 min at 12000 x g, 4 °C. The supernatant was removed and 0.5 vol % of 100% EtOH added. Subsequently, the RNA isolation with the Qiagen RNeasy kit was carried out. The columns provided were loaded with the RNA samples and spun at 3000 x g, 5 min at room temperature. To

achieve complete binding, the flow through was re-applied to the column in the same way. The column was washed with buffer RW1, and twice with RPE buffer (500 µl each). RNA was eluted with 2 x 20 µl H_20, and ethanol precipitated as described above for the L6 cells.

2.2.2.4 Large scale extraction of total RNA from heart tissue

Approximately 100 mg of frozen heart tissue was blotted dry, quickly placed into liquid nitrogen and immediately ground to a fine powder. The tissue powder was suspended in 2 ml Trizol reagent and homogenized with a small Potter Elvehjem–type glass homogenizer. The homogenate was incubated for 5 min at room temperature to permit the complete dissociation of nucleoprotein complexes. Chloroform (0.4ml) was added and the sample tube was capped securely, shaken vigorously for 15 s, and incubated at room temperature for 5 min. Following centrifugation at 12000 x g for 15 min at 4 °C, the upper aqueous phase was removed carefully, and placed into a fresh tube. While vortexing, 0.53 volumes of ethanol were added slowly to the supernatant. This mixture was loaded on an RNeasy midi column, and centrifuged at 3000 x g at room temperature for 5 minutes. The flow-through was poured back onto the column and spun again. The second flow-through was discarded. The column was washed twice with 4 ml RW1 buffer by centrifugation (5 min, 2800 x g). RNA was eluted from the RNeasy column with 150 µl DEPC treated water twice, and the

elute was mixed with 6 µl 3 M sodium acetate (pH 5.2) and 1 ml ethanol. After 15 minutes, RNA was pelleted by centrifugation (13000 x g at 4 °C for 15 minutes), and the pellet was washed twice with 75% ethanol. Following evaporation of the solvent (30 min in the fume hood), the RNA pellet was re-suspended in 20 µl DEPC treated water.

2.2.3 RNA integrity and quality assessment

2.2.3.1 Spectrophotometric and fluorometric detection of RNA

RNA quality was assessed using a spectrophotometer and a Fluorometer. The UV-absorbance at 260 and 280 nm of the RNA samples (diluted 1:100) was measured in a BioRad SmartSpec 3000 spectrophotometer. An OD_{260}/OD_{280} ratio between 1.8-2.0 was indicative of good quality RNA. Exact quantification of the RNA concentrations was done fluorometrically with RiboGreen (Amersham, USA) in a TD- 700 Laboratory Fluorometer (Turner Designer, USA), following the manufacturers instructions.

2.2.3.2 Electrophoresis

RNA quality was further analyzed by agarose gel electrophoresis. Two micrograms of total RNA were separated in a 1 % agarose gel, containing 0.5 ml

EtBr, and 0.9 ml 37 % formaldehyde. Electrophoresis was run for 30 min at 70 V in 1x MOPS buffer. The relative intensity of the ribosomal RNA bands was measured visually. A 28S:18S ratio of 2:1 indicated that the RNA quality was good, as illustrated in Fig. 2-1.

2.2.3.3 RT-PCR

RT-PCR was performed using primers specific for exon 2 and 3 of the rat fatty acid binding protein (FABP) gene in order to check the mRNA quality and the absence of genomic DNA contamination (upper primer R1, 5'-TAG CAT GAC CAA GCC GAC CAC AAT C-3', lower primer R4, 5'-GTT CCC GTG TAA GCT TAG TCT CCT G-3'). The RT-PCR product of the FABP mRNA should be 224 bp (Fig. 2-2), while genomic DNA contamination will result in a PCR product of 1 kb that includes intron 2.

RT-PCR beads (Amersham Pharmacia Biotech, Piscataway, NJ) were used. For a single 50 µl RT-PCR reaction, 500 ng total RNA was added. The primer concentration was 0.2 µM. The reverse transcription reaction was started by incubation for 10 min at 25 °C. Followed by 10 min at 60 °C and 15 min at 42 °C, the reverse transcription reaction was terminated by heating to 95 °C for 5 min and cooled to 4 °C. The PCR reaction was started by a denaturing step (95 °C for 1 min). The amplification proceeded for 31 cycles of 30 s at 95 °C, 30 s at 58 °C, and 1 min at 72 °C. The reaction mixture was then cooled down to 4 °C

and the products were separated on a 2% agarose gel. Detection was by ethidium bromide staining.

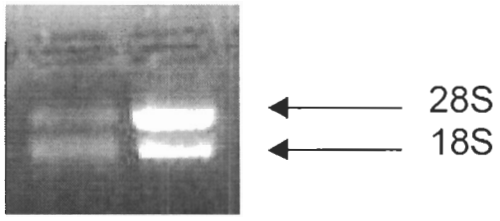

Fig. 2-1: RNA integrity assessment RNA samples on agarose gel

Purified RNA samples were separated by agarose gel electrophoresis, and the band intensities of the 18S and 28S subunits were measured. Lane 1 degraded RNA sample; 28S:18S ratio is less than 2:1.

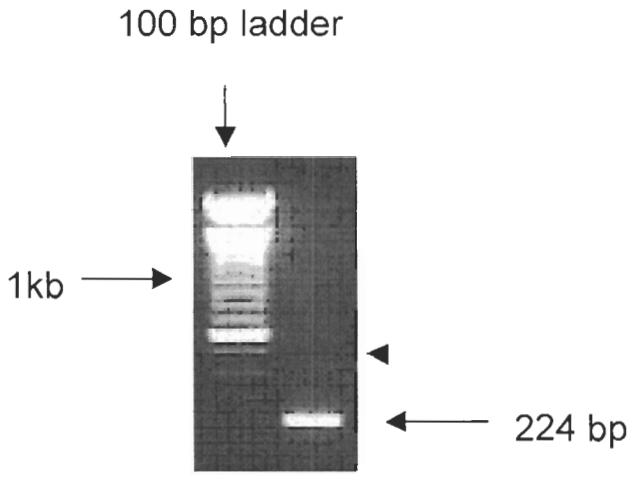

Fig. 2-2: RNA quality assessment by RT-PCR

Intact mRNA gives a 224 bp RT-PCR product (H-FABP primer R1 and R4 located on exon 2 and exon 3 of the FABP gene respectively). Genomic DNA contamination would give a 1kb RT-PCR product.

2.2.4 Probe preparation

2.2.4.1 'strip-able' cDNA probe (Ambion)

The Ambion method uses modified dATP to produce an easily 'strip-able' probe. Biotin-14-dATP is a dATP analogue which contains biotin attached at the 6–position of the purine base by a 14–atom spacer arm. This non-isotopic label was chosen as an alternative to the biotinylated dCTP in the Clontech procedure.

The following master mix was prepared for each reaction: 11 µl 5 x reaction buffer, 6 µl 10 x dNTP mix (Ambion's mix), 5.4 µl biotin-14-dATP and 2.1 µl DTT. The mixture was kept 10 min at 70 °C. Tubes were placed on ice for 1 min, and 2.5 µl of the PowerScript reverse transcriptase (Ambion) were added to the master mix and incubated for 5 min at 48 °C. The reaction tubes, containing 50 µg total RNA in up to 25 µl H_2O and 5 µl gene specific CDS-primer mix were treated for 10 min at 70 °C as well. The Clontech CDS-primer mix contains 1176 pairs of gene specific primers, which correspond to the DNA fragments fixed on the array membrane.

The master mix (20 µl) was added to the reaction with the total RNA, and kept at 48 °C. The reaction was stopped after 45 min by the addition of 1 µl 0.5 M EDTA.

2.2.4.2 Clontech cDNA probe with Atlas Spotlight Labelling Kit

The Atlas Spotlight Labelling kit generates biotin-labelled array probes from a minimum of 50 µg total RNA and gene specific CDS primers supplied with each Atlas array. This system uses biotinylated dCTP. A master mix was prepared for all labelling reactions plus 10 % extra. The following reagents per reaction were combined: 10 µl 5x reaction buffer, 5 µl 10 x labelling mix and 2.5 µl DTT (100 mM). The mixture was heated to 70 °C. For each reaction, 50 µg total RNA and 5 µl CDS primer mix was combined, brought with H_2O to a final volume of 30 µl, and incubated for 10 min at 70 °C. After the completion of a 5 min incubation at 48 °C, 2.5 µl Power Script reverse transcriptase was added to the master mix and incubated for 5 min at 48 °C. Subsequently, 20 µl of the master mix was added to each reaction tube and incubated for 45 min at 48 °C. The reaction then was stopped with 1 µl of 0.5 M EDTA.

2.2.4.3 Purification of the labelled probes

To separate the labeled cDNA from unincorporated biotin-labeled nucleotides and small cDNA fragments, the probes were diluted with 400 µl NT2 buffer and bound to small columns provided in NucleoSpin Extraction kit (Clontech, Mississauga). The probes were bound to the column, washed 3 times with a

washing buffer 500 µl NT3 buffer and then eluted from the column with 20 µl water.

2.2.4.4 Estimating the activity of biotin-labelled probes

The success of the labelling reaction was assessed via chemiluminescent detection, using the Clontech's SpotLight Chemiluminescent Hybridization & Detection kit. Dilutions of the Biotin dT100 Control with deionised water from a 10 ng/µl stock was prepared in a 1:5, 1:25, 1:125 and 1:625 ratio, and 1 µl each dilution was spotted onto a nylon membrane. The experimental probe was diluted 1:5 and spotted onto the membrane in the same volume. Following fixing the spotted samples by UV-cross linking, the membrane was blocked with blocking buffer (part of the Clontech kit). After 15 min, streptavidin–horseradish peroxidase conjugate (1:300 final dilutions) was added to the blocking buffer for 20 minutes. The membrane was washed with Wash I solution (2 X SSC, 1 % SDS) and placed for 5 min in a luminol/enhancer -and stable peroxidase solution. Signals were visualized on a sensitive BioMax ML Film (Kodak). The probe quality was assessed by comparing the signal strength with the oligo dT control; a 1:5 dilution of the probe resulted in a signal similar to Biotin dT100 at 1:125 (Fig. 2-3).

2.2.4.5 Array membrane pre- hybridization

SpotHyb buffer (Clontech) was gently warmed up to 45 °C until it appeared cleared. About 5µg of salmon testis DNA per probe was boiled for 5 min and then quickly chilled on ice. The DNA was added to 5ml pre-warmed SpotHyb buffer to make the prehybridization solution. Membranes were pre-hybridized in this solution at 42 °C for at least 2 h in hybrization tube.

2.2.4.6 Probe denaturing

While the membrane was pre-hybridizing, 1 M NaOH (1/10 of the total probe volume) was added to the array probe and incubated at 68 °C for 20 min. For every 50 µl original probe volume, 5 µl of C_0t-1 DNA and an equal volume of 2 x neutralizing solution (1 M NaH_2PO_4/pH 7.0) were added and incubated for another 10 min at 68 °C. The entire volume of freshly denatured biotinylated probe was added to the pre-hybridization mix, mixed well, and carefully pipetted into the hybridization bottle.

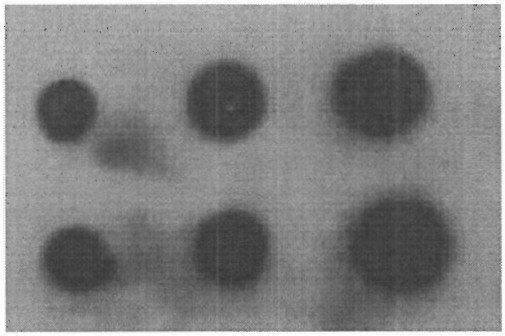

Fig. 2-4: Probe activity check using a homemade H-FABP dot blot

The H-FABP 224 base pair DNA fragment was blotted onto positively charged nylon membrane, and then used to check the activity of probes by hybridizing to this array. When the 2 ng spots showed good hybrization, the probe activity was considered to be adequate for macroarray hybridization.

2.2.4.7 Probe activity check with a "home-made" H-FABP dot blot

We chose an H-FABP-specific cDNA probe, which was synthesized with R1 and R4 primers from rat heart total RNA. Aliquots (2 ng, 10 ng, 50 ng) of the purified H-FABP DNA fragment (224 bp) were spotted onto a positively charged nylon membrane. The spots were air dried for 30 min, and then UV-light cross-linked for 1 min. The membranes were stored for subsequent use at -20 ^{0}C. An aliquot (10 %) of the denatured biotinylated probe (2.2.4.6) was used for the H-FABP specific membrane for probe activity check. Probes were used for the Clontech macroarrays if the 2 ng FABP spot showed up strongly after development (Fig. 2-4).

2.2.5 Hybridization procedure for Atlas Arrays

The denatured probe was hybridized to the atlas array membrane at 42 °C overnight with continuous gentle agitation. After hybridization the probe solution was poured off and stored in a Falcon tube at -20°C for re-use. The membranes were washed twice in 10–20 ml wash solution I (2 X SSC, 1 % SDS) for 30 min at 60 °C , and then twice for 20 min. The wash solution was replaced with wash solution II (0.1 % SSC, 0.5 % SDS) and incubated for 30 min at 48 °C.

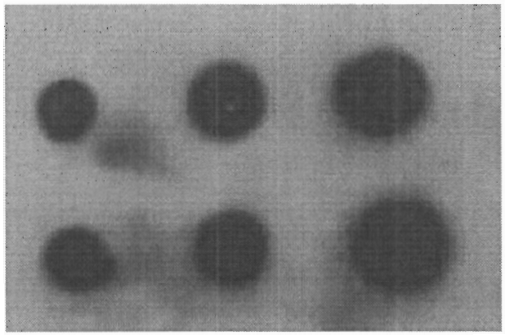

Fig. 2-4: Probe activity check using a homemade H-FABP dot blot

The H-FABP 224 base pair DNA fragment was blotted onto positively charged nylon membrane, and then used to check the activity of probes by hybridizing to this array. When the 2 ng spots showed good hybrization, the probe activity was considered to be adequate for macroarray hybridization.

2.2.6 Probe detection and signal visualization

The wash solution II was replaced with blocking buffer and incubated for 1 h at room temperature with gentle agitation. Streptavidin-HRP (83.3 µl) in 1 ml blocking buffer was added, and the incubation was continued for another 15 min. The membrane was washed 4 times for 10 min each with 1X wash buffer at room temperature, and then equilibrated for 5 min in substrate equilibration buffer. Equal volumes of the luminol/enhancer solution and the stable peroxide solution were mixed to form a working solution. Eight millilitres of this solution were spread evenly onto the membrane. The signals were developed for 5 min. The membranes were wrapped in Saran Wrap or plastic cover sheets and exposed to BioMax Light X-ray film for 10 sec, 30 sec, 1 min, 3 min, 5 min, 10 min, and 30 min. Figure 2-5 shows a 1 min exposure film.

2.2.7 Probe removal

2.2.7.1 "Easy strip-able probe" (Ambion) degradation and removal

Membranes were incubated for 5 min at room temperature with 1X probe degradation Buffer (Ambion), consisting of 100 µl 100 x degradation dilution buffer and 50 µl 200x probe degradation buffer in 10 ml water. Subsequently, the membrane was incubated for 20 min at 68 °C in reconstitution buffer (100 µl 20 % SDS, 100 µl 100x Blot Reconstitution buffer in 10 ml nuclease-free water).

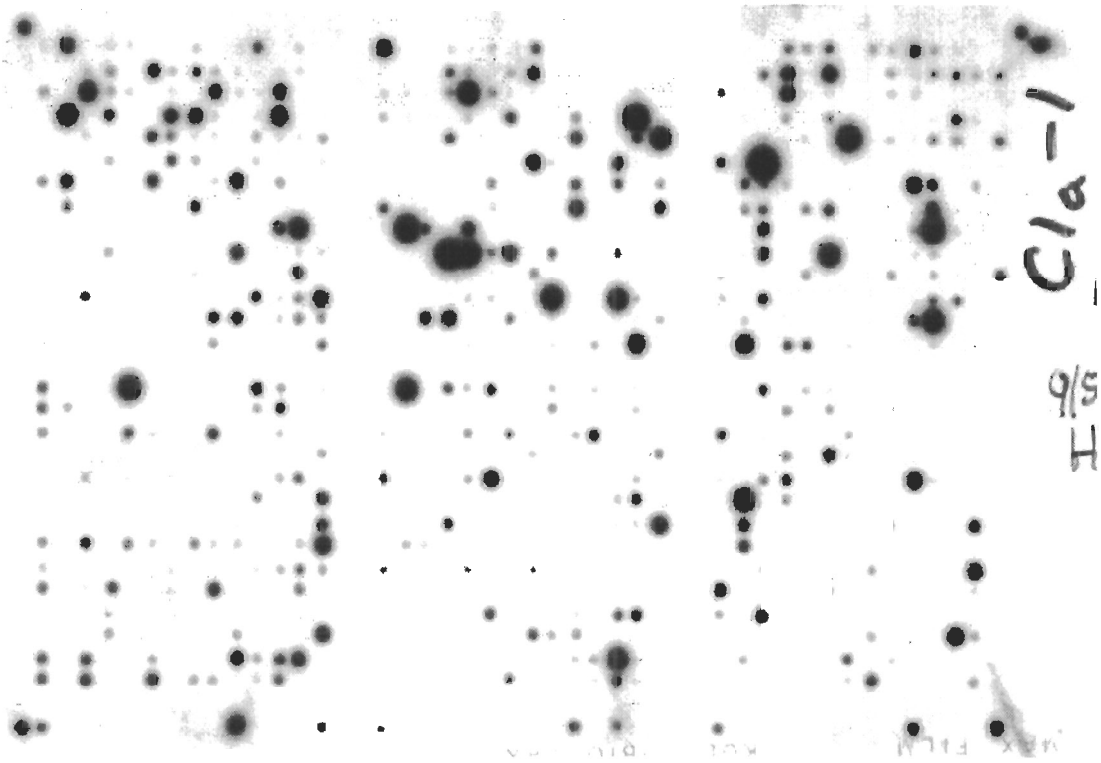

Fig. 2-5: Macroarray film of control rat heart

A macroarray was hybridized with a probe of control rat heart RNA, prepared using the Clontech protocol; the exposure time was 1-min.

To monitor the removal efficiency, the stripped membrane was treated again with luminol/enhancer and peroxidase solution, and exposed to X-ray film. Generally, no or only very weak signals (representing the strongest spots on the original blots) were detected; such weak signals did not interfere with subsequent experiments. The stripped membranes were stored in wash solution I at –20 °C; they were re-used more than 5 times.

2.2.7.2 Clontech probe degradation and removal

The Atlas Array membrane was washed twice for 15 min in 20 ml 0.1 % SDS solution in 0.2 N NaOH (stripping solution) at 37 °C, and rinsed in Wash Solution 1 (2X SSC, 1 % SDS) .The membrane background was checked by exposing the membrane to X–ray film. Following complete probe removal, the membrane was stored at -20 °C in a sealed plastic bag containing wash solution I. The membranes were re-used twice.

2.2.8 Image analysis

Films were scanned and analysed with BD Atlas Image^{TM} 2.7 (Clontech, California). For analysis of the array with Atlas software, I undertook the following steps to adjust and compare arrays from control and diabetic samples:

2.2.8.1 Aligning array to the grid template

I chose 2 anchor spots on the array and matched them to the corresponding spots on template. These two spots are diagonally opposed to each other, one on left bottom corner (an orientation spot) and another one located on right upper corner (another orientation spot). This distance between two spots made the alignment more precise.

2.2.8.2 Fine- tuning alignment

Atlas Image software designed the fine-tuning alignment function to allow adjusting of each gene spot perfectly to match the template. After overall alignment, I adjusted each individual gene spot on array to the specific spot on template. Fig. 2-6 shows the macroarray membrane after fine-turning alignment.

2.2.8.3 Background calculation

Atlas Image provides three options for calculating the background for the genes on array. When the array looked clear and even, I chose default external background calculation method, which is set at the median intensity of the blank space between different panels of the array. When an array had a splotchy and

uneven background, I used the local background calculation method, which is based on the median intensity of the space directly surrounding the gene spots, located in the splotchy area.

2.2.8.4 Negative and positive controls in the macroarray experiment

Atlas Image Rat Macroarrays are designed to have both negative and positive control spots on the array. Plasmid and bacteriophage DNAs, M13 mp 18(+) strand DNA, lambda DNA, pUC 18 DNA, are designed on Atlas Rat array membrane as negative controls to confirm hybridization specificity.

2.2.8.5 Signal threshold

Atlas Image is designed to adjust the threshold level, which is the signal level required to be considered a real spot. The threshold was set at 2 X background signal, thereby filtering out weak signal spots.

2.2.8.6 Averaging multiple arrays

Atlas Image software averages up to 8 replicated experimental arrays. I replicated 3 control rat heart and 3 diabetic rat heart macroarray experiments and averaged all my replicated 3 experiments results. For each macroarray

experiment, independently extracted RNA samples from different animals were sued to make the probe.

Comparing diabetic rat heart array with control rat heart array: the Atlas Image comparison tools allowed calculating the ratio of each gene changes. We obtained the ratio of the diabetic gene spot signal divided by control gene spot signal. Adjusted intensities equal the gene spot signal minus the background value and then multiplied by the normalization coefficient.

$$\text{Normalization Coefficient} = \frac{\text{(Intensity-background) housekeeping gene of Array 1}}{\text{(Intensity-background) housekeeping gene of Array 2}}$$

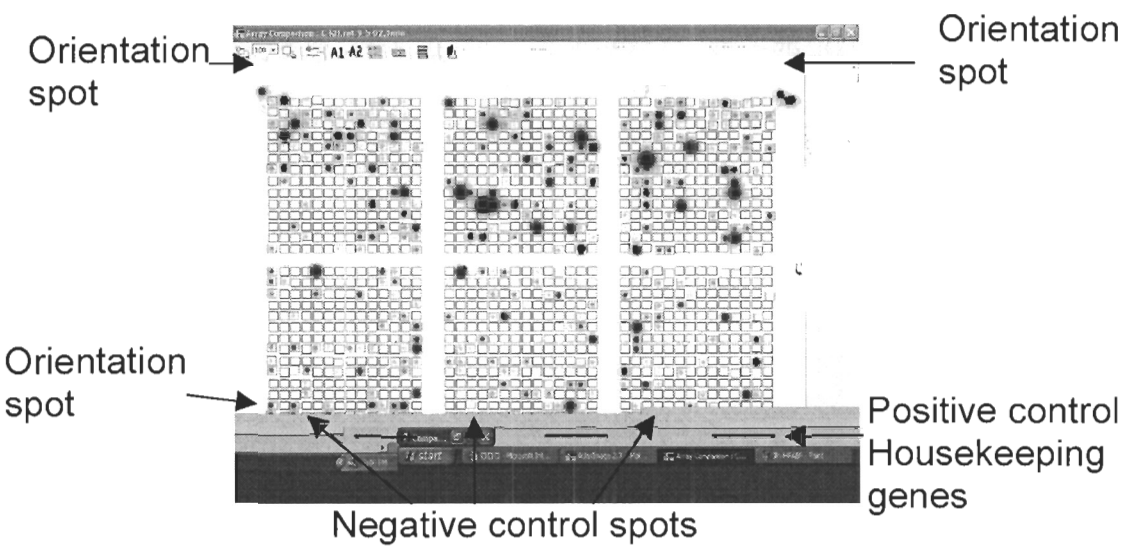

Fig. 2-6: Macroarray film after fine aligning

The macroarray film image was adjusted with the Atlas Image software. Fine tuning alignment was used to adjust each gene spot on the array perfectly match the template (square boxes).

2.2.9 Normalizing the array

It is important to normalize the signal intensity between the two arrays because these two arrays vary even under the same conditions. To normalize two arrays, we identified housekeeping genes, which generated equally intense signals for both samples. Atlas Image provides three normalization methods: Global normalization, which has the "sum"-method and "median" -method, and a user-defined normalization method. In my experiment, I chose the user-defined normalization method. I chose housekeeping genes — (GAPDH, beta actin, 40S ribosomal protein S29) then calculated the two intensity values and divided them to get the normalization coefficient. Finally, all housekeeping genes normalization coefficients were averaged to obtain an array normalization coefficient, which was used to normalize two arrays.

2.3 Results

The macroarrays probed with the 'strippable' probe (Ambion) (Fig. 2-7) showed uneven spots. Some spots appeared very large and strong, while others seemed very faint. Generally, the arrays resulted in very high contrast images, with less graduated signals than those obtained with the Clontech probes (Fig. 2-8). This

resulted in much higher differences between strongly and weakly expressed genes. It was found that the concentration of biotinylated dATP was limiting for the reverse transcription. As more concentrated biotinylated dATP was not commercially available, the strippable probes were not suitable for this quantitative data, and all subsequent macroarrays were hybridized to probes made using the Clontech protocol.

From the comparison of control and diabetic rat heart (Fig. 2-8, Fig. 2-9), the S29 (Fig. 2-10) and β-actin spot intensities did not change significantly; therefore, the average intensities of these housekeeping genes was used to normalize the control and diabetic array films. Table 2-1 and 2-2 show the differences between control and diabetic rat heart found with the macroarray experiments using probes prepared using the Clontech protocol. At least 154 genes were found to change during STZ-induced diabetes: 130 down-regulated genes and 24 up-regulated genes. Down-regulated genes include several ion channel and signal transduction proteins, while various proteins involved in fatty acid metabolism appear to be up-regulated. The significance of these results will be discussed further in Chapter 4.

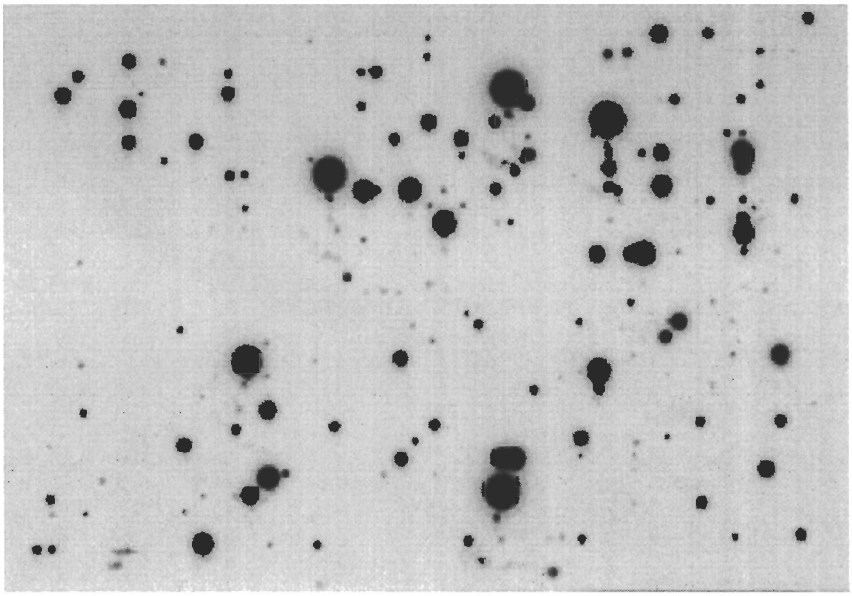

Fig. 2-7: The film resulting from hybridization with the Ambion probe

Hybridization of Ambion probe to macroarray film resulted in uneven spots on the membrane. Some spots were very large, while some smaller spots disappeared while compared to Clontech probe membrane (Fig. 2-8). Exposure time was 1 min.

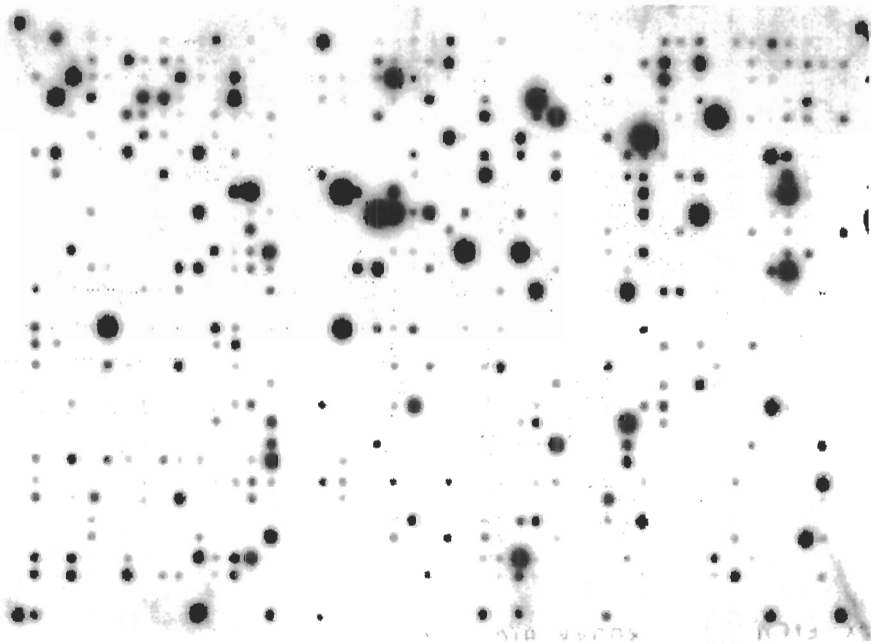

Fig. 2-8: Macroarray of control rat heart gene expression

A macro array was hybridized with a Clontech probe prepared from 50 µg control heart RNA. Exposure time was 1 min.

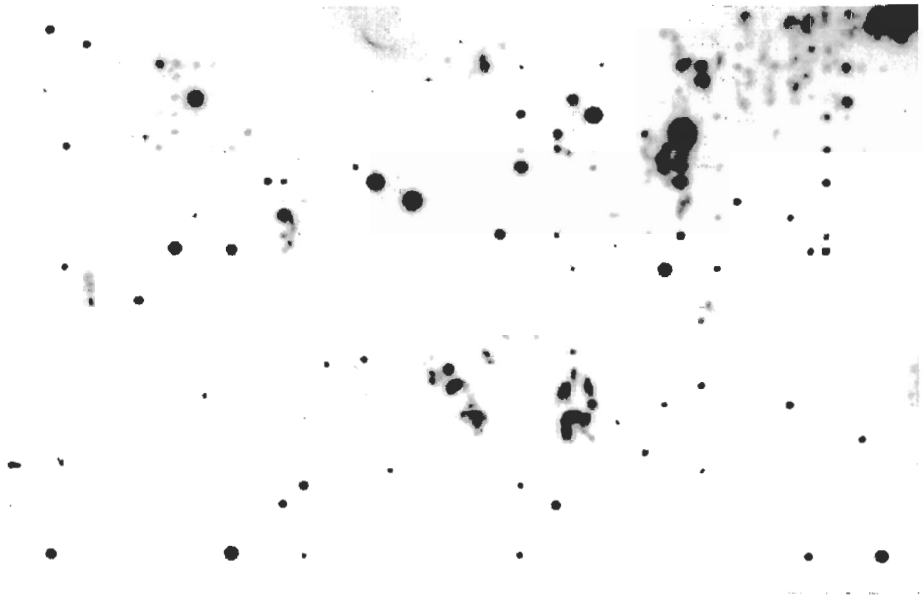

Fig. 2-9: Macroarray of diabetic rat heart gene expression

A macro array was hybridized with a Clontech probe prepared from 50 µg diabetic heart RNA. Exposure time was 1 min.

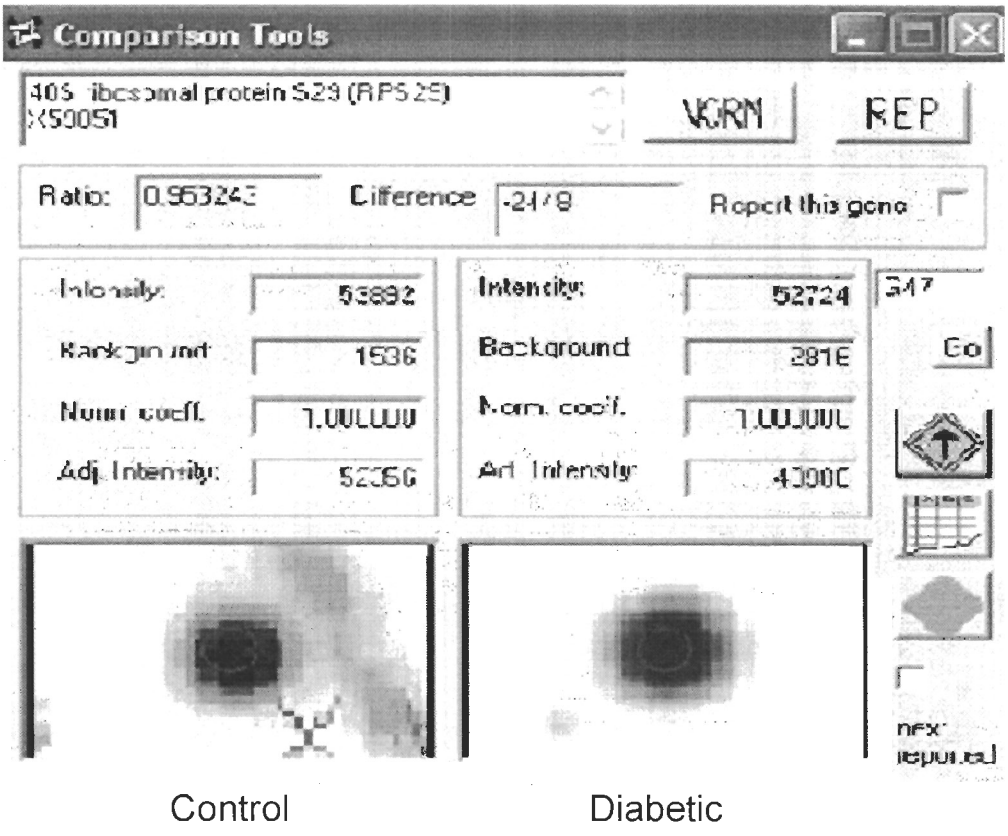

Fig. 2-10: Comparison of band intensities of the S29 ribosomal RNA

From the comparison of control and diabetic rat heart, the spot intensity ratio was found to be 0.95, indicating that S29 could be used as housekeeping gene in subsequent macroarray experiments.

Table 2-1: Genes down-regulated in diabetic animals

Genbank ID	Protein/gene	control [pixels]	diabetic [pixels]	ratio°
M55291	BDNF/NT-3 growth factor receptor precursor; trkB tyrosine kinase; gp145-trkB/gp95-trkB; NTRK2	44407	49	0.00
L27128	c-Jun N-terminal kinase 3 (JNK3); stress-activated protein kinase beta (SAPK-beta)	23540	191	0.01
X66974	calretinin	51425	424	0.01
M95735	syntaxin B	29721	247	0.01
L19698	Ral A; GTP-binding protein	34504	318	0.01
M60525	VGF8A protein precursor	26848	252	0.01
U69278	Rek4 Eph-related receptor tyrosine kinase; ephrin type-A receptor 3; EphA3; similar to Etk1	46531	505	0.01
L31620	acetylcholine receptor, nicotinic, alpha 4	28763	324	0.01
D37920	squalene monooxygenase; squalene epoxidase (SQLE; SE); ERG1	32639	393	0.01
J02762	asialoglycoprotein receptor R2/3 (ASGPR); hepatic lectin 2/3; RHL-2	28631	358	0.01
J02627	cytochrome P450 2E1 (CYP2E1); P450-J; P450RLM6	14940	213	0.01
M34184; M15191; M34183	protachykinin alpha precursor (alpha-PPT); substance P + protachykinin beta precursor (beta-PPT); neurokinin A; substance K; neuromedin L; neuropeptide K + protachykinin gamma precursor; substance P	25309	406	0.02
J04563	DPDE4; cAMP-dependent 3',5'-cyclic phosphodiesterase 4B	17839	315	0.02
M37482	inhibin, beta A subunit	22643	404	0.02
U48245	protein kinase C-binding protein nel homolog 1	32208	619	0.02
U28927	liver Na+/Cl- betaine/GABA transporter	13640	265	0.02
AF010464	interleukin-7 (IL-7)	21709	422	0.02
M34097	natural killer (NK) cell protease 1 (RNKP-1)	52104	1025	0.02
M55250; M38385	glycine receptor alpha 3 subunit precursor (GLRA3)	49625	1012	0.02
U09540	P450 IB1; C3H cytochrome P450; CYP1B1	56155	1191	0.02
U23443	PAK-alpha serine/threonine kinase; p21-Cdc42/Rac1 activated kinase; p68-PAK; MUK2	12004	273	0.02
L38247	synaptotagmin IV (SYT4)	17036	409	0.02
S68944	sodium/chloride neurotransmitter transporter	12495	307	0.02
X59290	eek proto-oncogene, protein tyrosine kinase, eph/elk-related	14376	361	0.03
L77929	G-protein activated K+ inward rectifier	17003	442	0.03

J04629	**sodium/potassium-transporting ATPase beta 2 subunit (ATP1B2)**	13052	343	0.03
M19651	fos-related antigen 1 (FOSL1; FRA1)	11100	298	0.03
M59980	**voltage-gated K+ channel protein; RK5; potassium channel protein**	47968	1423	0.03
D14051	**inducible nitric oxide synthase (iNOSI); type II NOS**	5476	170	0.03
M55050	interleukin-2 receptor beta chain	9757	315	0.03
L05175	granzyme M precursor (GZMM); MET-ASE; natural killer cell granular protease; RNK-MET-1	21880	714	0.03
X69903	interleukin-4 receptor	33803	1143	0.03
U92802	G-protein coupled receptor, putative, GPR41	9231	319	0.03
M55049	interleukin-2 receptor alpha subunit precursor (IL-2 receptor alpha; IL2RA); TAC antigen; CD25 antigen	21067	733	0.03
U61373	proteinase activated receptor 2 precursor (PAR-2)	53659	2110	0.04
X74832	acetylcholine receptor alpha	33759	1394	0.04
M12492	cAMP-dependent protein kinase type II-beta regulatory chain	8529	357	0.04
L23088	P-selectin precursor; granule membrane protein 140 (GMP-140); PADGEM; CD62P; leukocyte-endothelial cell adhesion molecule 3 (LECAM3)	57055	2431	0.04
Y10369; Y10370	GABA-B receptor 1a (GABA-BR1A receptor) + GABA-B receptor 1b (GABA-BR1B receptor)	25311	1221	0.05
Z14119	platelet-derived growth factor receptor, alpha	24349	1252	0.05
Z11558	glia maturation factor beta (GMF-beta; GMFB)	33741	1809	0.05
X61479	c-fms proto-oncogene; macrophage colony stimulating factor 1 (MCSF-1) receptor	17289	933	0.05
M18335; J03509; M18774	cytochrome P450 2C7 (CYP2C7); P450F; PTF1	59296	3220	0.05
D84667	PI4-K; phosphatidylinositol 4-kinase (92/100 kDa, soluble)	58416	3226	0.06
J02999	ras-related protein Rab2	16809	937	0.06
D21799	proteasome subunit RC7-I	55985	3185	0.06
M18330	**protein kinase C delta type (PKC-delta)**	26349	1509	0.06
L04796	glucagon receptor precursor (GL-R)	24712	1434	0.06
D10728	T-cell surface glycoprotein CD5 precursor; lymphocyte glycoprotein LY-1 (LYT1)	55065	3274	0.06
D10026	glutathione S-transferase, Yrs-Yrs inactivating	55839	3376	0.06
L23219	guanine nucleotide-binding protein G(I)/G(S)/G(O) gamma-7 subunit (GNG7; GNGT7)	24347	1493	0.06
U89529	fatty acid transport protein	8569	575	0.07

M80633	adenylyl cyclase 4	37853	2635	0.07
J03025	muscarinic acetylcholine receptor M2	32340	2371	0.07
U76205	scavenger receptor class B type I	9133	676	0.07
M88111	high affinity L-proline transporter	43105	3372	0.08
D45187	cathepsin E	16148	1293	0.08
AF003926	ovalbumin upstream promoter gamma nuclear receptor rCOUPg	28813	2611	0.09
D10021	mitochondrial ATP synthase D subunit; ATP5H	17504	1587	0.09
M86621	**calcium channel, L-type, dihydropyridine-sensitive, alpha 2 subunit**	48512	4478	0.09
X62660; S37370	glutathione transferase, subunit 8	10880	1031	0.09
X59132	secretin receptor	42112	4182	0.10
D21158	thromboxane A2 receptor (TBXA2R; TXR2); prostanoid TP receptor	15211	1521	0.10
L20820	syntaxin 3 (STX3)	5405	544	0.10
M69139	SR13 myelin protein; peripheral myelin protein 22 (PMP-22); CD25 protein	8345	867	0.10
U05675	fibrinogen beta subunit (FGB)	28251	3047	0.11
M12516	**NADPH-cytochrome P450 reductase (CPR); POR**	13876	1579	0.11
X74806 + X52016	von ebner's gland protein 2; VEG protein 2; VEGP2 + von ebner's gland protein 1; VEG protein 1; VEGP1; VEGP	39709	4705	0.12
L35572	Lim-2; embryonic motor neuron topographic organizer, HOMEOBOX PROTEIN LIM-2 (LIM/HOMEODOMAIN PROTEIN LHX5).	28617	3523	0.12
M91808	**sodium channel, beta 1 subunit**	26891	3620	0.13
X77933	**sodium channel SHRSPHD, gamma subunit, epithelial**	38233	5279	0.14
U05341	p55cdc; cell division control protein 20	3712	538	0.14
U16253	corticotropin-releasing factor receptor subtype 2 (CRF2R)	10381	1515	0.15
M67465	3-beta hydroxy-5-ene steroid dehydrogenase type III (3beta-HSD III; EC 1.1.1.145); steroid delta-isomerase (EC 5.3.3.1); progesterone reductase	26648	4101	0.15
S69323	neurotrophin 5, trk and trkb activating	59227	9781	0.17
X58023	corticotropin-releasing factor binding protein	35799	5995	0.17
D14015	Cyclin E	34625	5824	0.17
L15619	casein kinase II beta subunit (CKII; CSNK2B; CK2N); phosvitin	54215	9192	0.17
AF007836	RIM; Rab3 effector in synaptic-vesicle fusion	24407	4147	0.17
X78327	ribosomal protein L13	42075	7292	0.17
M22412	ISK slow voltage-gated potassium channel protein; mink potassium channel; KCNE1	58863	10271	0.17
U72487	calcium-independent alpha-latrotoxin receptor	13597	2489	0.18

X70871	G2/M-specific cyclin G (CCNG)	19796	3794	0.19
M91590	beta-arrestin 2 (ARRB2)	42023	8369	0.20
D88666	serine phospholipid-specific phospholipase A; PS-PLA1 precursor	19243	4091	0.21
X06942	A-raf proto-oncogene	24733	5350	0.22
U52825	syndecan 3	49769	11091	0.22
L31771	alpha-1D adrenergic receptor (ADRA1D); alpha 1D-adrenoceptor; alpha-1A adrenergic receptor (ADRA1A); RA42	31893	7133	0.22
M85299	sodium/hydrogen exchange protein 1	46091	11418	0.25
D32249	NEURODEGENERATION ASSOCIATED PROTEIN 1; downregulated by axotomy	14844	3701	0.25
D10862	DNA-binding protein inhibitor ID1	29597	7380	0.25
D17615	14-3-3 protein zeta/delta; PKC inhibitor protein-1; KCIP-1; mitochondrial import stimulation factor S1 subunit	23580	6256	0.27
AF019973	neuron-specific enolase (NSE); gamma enolase (EC 4.2.1.11); 2-phospho-D-glycerate hydrolyase	3517	964	0.27
L26043	perilipin A/B (PERIA/PERIB); lipid droplet-associated proteins A/B	22203	6425	0.29
X17163	c-jun proto-oncogene; transcription factor AP-1; RJG-9	30392	9006	0.30
M90398	ATPase, hydrogen-potassium, alpha 2a subunit	36193	10752	0.30
X56917	1D-myo-inositol-trisphosphate 3-kinase A (ITPKA); inositol 1,4,5-triphosphate 3-kinase (IP3 3-kinase; IP3K)	52297	15864	0.30
U31367	MAL; T-lymphocyte maturation-associated protein; myelin protein MVP17	35900	11075	0.31
D89863	ras-related protein m-ras	23825	7358	0.31
U62803	lecithin:cholesterol acyltransferase (EC 2.3.1.43; LCAT); phosphatidylcholine-sterol O-acyltransferase; phospholipid-cholesterol acyltransferase	40497	12640	0.31
X06769	c-fos proto-oncogene	35352	11389	0.32
U29339	ErbB3 EGF receptor-related proto-oncogene; HER3	25437	8516	0.33
J03624	galanin precursor (GALN; GAL)	19388	6523	0.34
M92905	calcium channel, alpha 1 beta	60873	21523	0.35
U37138	steryl-sulfatase precursor (EC 3.1.6.2); steroid sulfatase; steryl-sulfate sulfohydrolase; arylsulfatase C (ASC)	22179	7958	0.36
D85760	guanine nucleotide-binding protein alpha 12 subunit (G alpha 12; GNA12)	38732	14118	0.36
L19660	gastric inhibitory polypeptide receptor precursor (GIP-R); glucose- dependent insulinotropic polypeptide receptor	24615	8972	0.36
D28753 + D28754	cyclin-dependent kinase 2 alpha (CDK2-alpha) + cyclin-dependent kinase 2-beta (CDK2-beta)	18004	6685	0.37
U46034	stromelysin 3; matrix metalloproteinase 11 (MMP11)	26181	10032	0.38

M93669	secretogranin II precursor (SGII; SCG2); chromogranin C (CHGC)	57317	22264	0.39
D16817	metabotropic glutamate receptor 7 precursor (GRM7; MGLUR7)	29935	11651	0.39
D42145	ATP-sensitive inward rectifier potassium subfamily J member 8 (KCNJ8); UKATP-1; ATP-sensitive inwardly rectifying K+ channel KIR6.1	22169	9408	0.42
X15030	cytochrome c oxidase, subunit Va, mitochondrial	50887	22181	0.44
M96377+ M96376	Non-processed neurexin II-beta major, NEUREXIN II-BETA-A PRECURSOR + Non-processed neurexin II-alpha, NEUREXIN II-ALPHA-B PRECURSOR	17913	7935	0.44
X77797	interleukin 8 receptor	27100	12052	0.44
D45201	neurofibromin; neurofibromatosis protein type I (NF1); GTPase stimulatory protein	57979	26270	0.45
D25290	cadherin 6 precursor; kidney-cadherin (K-cadherin)	26649	12606	0.47
M36589	beta-nerve growth factor precursor (beta-NGF)	55111	26674	0.48
L11004	sodium-hydrogen exchange protein-isoform 2 (NHE-2)	49403	23961	0.49
M27925	synapsin 2A	58869	28663	0.49
X87106	ribosomal protein L10	59439	29475	0.50
M21208	cytochrome P450 17 (CYP17); P450C17; CYPXVII; steroid 17-alpha-hydroxylase/17,20 lyase	58721	30001	0.51
J02650	60S ribosomal protein L19 (RPL19)	59561	30625	0.51
M20637	phospholipase C delta 1 (PLC delta-1); PLC-III	35040	18271	0.52
D10854	NADP+ alcohol dehydrogenase; aldehyde reductase (ALR); 3-dG-reducing enzyme	49813	27407	0.55
U94708	prostaglandin E2 receptor EP2 subtype (PGE receptor EP2 subtype; PTGER2); prostanoid EP2 receptor	58717	32439	0.55
U28356	HEP; LC-PTP protein-tyrosine phosphatase; hematopoietic protein-tyrosine phosphatase (HEPTP)	36669	20539	0.56
Y14019	Rab-3b ras-related protein	46925	28023	0.60
D83538	PI4-K; phosphatidylinositol 4-kinase (230 kDa)	19940	12642	0.63
X13817	calmodulin (CALM; CAM)	32597	21895	0.67
M89791	**insulin-like growth factor binding protein 1 precursor (IGFBP-1; IBP-1)**	20019	13907	0.69

°Ratio was determined by comparing spot intensities (average of 3 from control and diabetic samples). Bold printed genes are discussed further in this thesis. Ratio < 0.5 generally is considered significant, with higher ratios only showing a trend.

Table 2-2: Genes up-regulated in diabetic animals

Genbank ID	Protein/gene	control [pixels]	diabetic [pixels]	Ratio*
J02791	**medium chain acyl-CoA dehydrogenase precursor (MCAD; ACADM)**	24281	27857	1.15
D13123	ATP synthase lipid-binding protein P1 precursor; ATPase protein 9; ATP5G1	28487	37828	1.33
D13126	NVP-3; neural visinin-like Ca2+-binding protein, VISININ-LIKE PROTEIN 3 (VILIP-3) (NVP-3).	11768	15786	1.34
X01118	natriuretic peptide precursor, gamma, atrial	13407	18600	1.39
L03294	lipoprotein lipase precursor (LPL)	8920	13257	1.49
D17512	cysteine-rich protein 2 (CRP2); ESP1	29517	44171	1.50
M21730 J03898	annexin V (ANX5); lipocortin 5; placental anticoagulant protein I (PAP-I)	9143	14198	1.55
M18547	40S ribosomal protein S12	11391	18776	1.65
K03502	elongation factor 2 (EF2)	13043	22805	1.75
X12554	cytochrome c oxidase, subunit VIa, heart	19709	35421	1.80
J03960	arachidonate 5-lipoxygenase (EC 1.13.11.34); 5-lipoxygenase (5-LO)	19789	36040	1.82
M62388	UBE2B; ubiquitin-protein ligase; ubiquitin carrier protein;	5817	10604	1.82
D90109	**long chain acyl-CoA synthetase 2 (LACS2); long chain fatty acid-CoA ligase**	34508	66712	1.93
AF072411	**platelet glycoprotein IV; GPIIIB; CD36 antigen; fatty acid translocase (FAT)**	13049	27630	2.12
K03250	40S ribosomal protein S11	6611	14871	2.25
AF16297	neuropilin 2	12557	30074	2.39
J05029	**long chain-specific acyl-CoA dehydro-genase precursor (LCAD; ACADL)**	12349	30300	2.45
J05470	**mitochondrial carnitine O-palmitoyltransferase II precursor (CPT II)**	3189	9709	3.04
D10874; D01244	vacuolar ATP synthase 16-kDa proteolipid subunit; ATP6C; MVP; ATPL	993	4096	4.12
L29259	elongation factor SIII P15 subunit	611	7233	11.84
U11760	ATPase, transitional endoplasmic reticulum	1184	14719	12.43
J04503	protein phosphatase 2C alpha (PP2C alpha; PP2C1); protein phosphatase 1A (PPM1A)	295	3672	12.43
S90449	protein phosphatase 2C isoform; Mg2+ dependent protein phosphatase beta isoform	781	11919	15.27
U34958	transducin beta-1 subunit; GTP-binding protein G(i)/G(s)/G(t) beta subunit 1	378	8723	23.08
D30647	**very long chain acyl-CoA dehydrogenase (VLCAD) ****	984	29602	30.08
M14201	**11-kDa diazepam binding inhibitor (DBI), acyl-CoA binding protein; ACBP****	552	17176	31.12

*Ratio was determined by comparing spot intensities (average of 3 from control and diabetic samples). Bold printed genes are discussed further in this thesis. Ratio > 2 generally is considered significant, with lower ratios only showing a trend. **These genes were taken from Atlas rat toxicology array; one experiment only.

Table 2-3: Genes highly expressed in control and diabetic animals

Genbank ID	Protein/gene	control [pixels]	diabetic [pixels]	Ratio *
D16554	polyubiquitin	56996	46549	0.82
J02773	**fatty acid-binding protein (heart; H-FABP)**	58812	48064	0.82
J04022	ATPase, calcium, brain	55731	39555	0.71
M94043	Rab-related GTP-binding protein	57956	43625	0.75
X16956	microglobulin; beta-2-microglobulin + prostaglandin receptor F2a	52832	47935	0.91
AF000423	SYNAPTOTAGMIN XI; membrane trafficking protein	59840	46346	0.77
J05231	neuronal acetylcholine receptor protein alpha 5 subunit precursor (CHRNA5; ACRA5)	60397	47899	0.79
M16410	NEUROKININ B PRECURSOR (NEUROMEDIN K)	54716	40171	0.73
M28647	Na+/K+ ATPase alpha 1 subunit	59944	42718	0.71
M64373	voltage-dependent P/Q-type calcium channel alpha-1A subunit (CACNA1A); L type calcium channel alpha-1 polypeptide isoform 4 (CACNL1A4; CACH4); brain calcium channel I; rat brain brain class A (RBA-1); CACN3	60807	48023	0.79
S79304	cytochrome oxidase, subunit I, Sertoli cells	60441	48172	0.80

*Ratio was determinined by comparing spot intensity (average of 3 from control and diabetic samples). Bold printed genes are discussed further in this thesis. The spots for these genes are near saturation for both control (~55000 pixels) and diabetic animals (~45000 pixels after normalization). It is therefore impossible to decide whether these genes are up- or down-regulated.

2.4 Discussion

High quality, intact RNA is the first and most critical factor for reliable gene expression analysis. RNA stabilization is an absolute prerequisite for many fundamental molecular biology experiments. Any RNA degradation must be avoided, especially for quantitative real time PCR and gene array experiments. We have tried several RNA extraction methods and various kits to get good quality RNA from rat heart tissue. Heart muscle is a difficult tissue for RNA isolation due to the abundance of contractile proteins, connective tissue, and collagen. We found that the best way to extract RNA from heart tissue is to use a combination of the Trizol reagent method and the Qiagen RNeasy kit. Initially, the Trizol reagent removes connective tissue and most of the proteins, and then the Qiagen Kit is useful to remove residual protein and DNA contamination. This combined method yielded sufficient amounts of high quality RNA that meet the requirements of macroarray and real time PCR experiments (see Chapter 3).

The use of high-quality, pure RNA is essential for obtaining reproducible gene expression data. However, RNA is not stable and is easily degraded. Repeated freezing and thawing of RNA samples leads to degradation of the RNA sample, which then would contain incomplete gene information. Storage of RNA samples at below –70 °C is essential. The best way to avoid any degradation caused by

freezing and thawing is to use freshly extracted RNA. In my experiment, I used freshly extracted RNA for the macroarray experiments.

Reproducible results in the macro array experiments depended on various parameters, including normalization techniques and the quality of the RNA/cDNA samples. Normalization is necessary in macroarray experiments since the absolute amounts of mRNA cannot be determined, due to variations in labelling, hybridization, spotting, or surface characteristics of different batches of membranes. Expression intensities resulting from the same amount of mRNA can differ when comparing two macro array membranes. There are two different methods used for the normalization between different membranes, global normalization and the use of individual housekeeping genes. The global normalization selects all genes signal values, and normalizes each value based on the total signal intensities. This method is suitable when only a few genes are differentially expressed, but most genes stay the same. Housekeeping genes, on the other hand, are preferred when the expression of many genes changes and the total signal intensity is not constant. In my experiment, while considering that diabetic disease actually affects the whole energy metabolism and numerous associated enzyme and signal transduction pathways, one would expect many differences between diabetic and control hearts. Indeed, from the films of diabetic samples it was apparent that many genes are down-regulated, with some spots completely disappearing. In this case, global normalization is not suitable. Therefore, we chose a user defined housekeeping gene method to normalize

between arrays. It is, however, critical to select housekeeping genes that are definitely not affected by the diabetic condition. This is a problem, since no studies exist that conclusively prove unaltered expression of specific housekeeping genes and must be kept in mind when evaluating the results.

Another potential source of errors is the procedure of collecting heart sample. Samples prepared from whole heart left ventricle tissue contains both heart tissue and connective tissues; even though 65 % - 80 % of the heart are cardiomyocytes, there are considerable amounts of other cells, including epithelial cells and cardio-adipocytes (Montford and Perez-Tamayo, 1962). Variations in their relative proportions in the sample will influence the intensity of their messages, which may be falsely interpreted as gene expression changes. This problem can be avoided by studying only myocytes. Myocyte isolation, however, is time consuming and stressful to the cells, which could lead to many gene expression changes unrelated to the underlying disease. Laser capture microdissection (LCM) has been used (Emmert-Buck et al., 1996) to extract a pure subpopulation of heart muscle cells from the heart ventricle. The combination of LCM with microarray and real time PCR could provide a crucial step forward to investigate gene expression profiles in diabetes, but LCM was not available to us. Moreover, it may be difficult to get enough cells to produce the amounts of RNA required for the array experiments.

Because of these limitations, our macroarray experiments only provide a semi quantitative assessment of potential gene expression change in diabetic rat hearts. When comparing control and diabetic samples, most genes appear to be down-regulated in diabetic rat hearts. However, fatty acid metabolism related genes, such as fatty acid binding protein (FABP), acyl-CoA dehydrogenases, or CPT, have been reported to be up-regulated. In all macroarray experiments, a strong saturated spot was obtained for FABP in both control and diabetic samples that mean that possible up-regulation cannot be reliably quantified. Several other genes, however, show clearly up-regulation: long chain acyl-CoA dehydrogenase, medium chain acyl-CoA dehydrogenase, very long chain acyl-CoA dehydrogenase, CPT, and Acyl-CoA synthetase (ACS) all showed stronger spots after normalization. As discussed further in Chapter 4, the up-regulation of these genes may be the direct result of the increased cellular fatty acid content, and thus we were mostly interested in these genes. Because of the possible errors and variations discussed above, their mRNA levels need to be verified by a more accurate method. To quantify gene changes more accurately, real time PCR was used to investigate these fatty acid related genes.

CHAPTER 3: MONITORING THE EXPRESSION CHANGES OF SELECTED GENES USING QUANTITATIVE REAL-TIME PCR

3.1 Introduction

Real-time reverse transcription polymerase chain reaction (qRT-PCR) is a highly sensitive, reproducible method used to detect and quantify gene expression. Compared to other currently-used methods for the quantification of gene expression, such as Northern blot hybridization, ribonuclease protection assays and competitive quantitative RT-PCR, qRT-PCR assays provides a more accurate and reproducible quantification of results because it measures the amount of PCR product generated during the exponential phase of the PCR (Wood, 2002). Therefore, qRT-PCR is increasingly used to quantify changes in gene expression. For example, Aerts and coworkers used real time PCR to study genes changes in tumor antigens (Aerts et al., 2004).

A key component of qRT-PCR is SYBR Green I dye, which binds in the minor groove of double-stranded DNA in a sequence-independent way, and once bound, its fluorescence increases over 100-fold (Lekanne Deprez et al., 2002). Initially, the number of cycles necessary to detect a fluorescence signal is

determined (threshold cycle number), which is the starting point for measuring the accumulation of the gene specific PCR product. The subsequent increase in fluorescence is proportional to the gene-specific cDNA present in the sample.

My previous gene macroarray experiments gave me an estimate in diabetic rat heart of the expression levels changes of hundreds of different genes. We chose qRT-PCR to confirm the up regulation of selected genes from the macroarray results specially those involved in fatty acid metabolism, including heart fatty acid binding protein (H-FABP), long-chain acyl–CoA synthetase (ACS), mitochondrial muscle carnitine O-palmitoyltransferase (CPT), medium-chain acyl-CoA dehydrogenase (MCAD), long-chain acyl-CoA dehydrogense (LCAD), very-long-chain acyl-CoA dehydrogenase (VLCAD), and acyl-CoA binding protein (ACBP) (see table 2-2 or 2-3). This study allowed us to validate the macroarray results, provided more accurate and reliable data on their expression changes in the heart of diabetic rat, compared to normal animals.

3.2 Material and methods

3.2.1 Materials

RNeasy Midi Kits were obtained from Qiagen (Mississauga, Ontario), SYBR Green I from Invitrogen (Toronto, Ontario). PCR experiments were carried out with Ready-To-Go RT-PCR beads and Ready-To-Go PCR beads (Amersham

Pharmacia Biotech, Toronto, Ontario). All other chemicals were of analytical grade and purchased from Sigma (Toronto, Ontario) or Gibco (Toronto, Ontario). RNAlater was purchased from Ambion (Austin, Texas).

3.2.2 Methods

3.2.2.1 Total RNA extraction

Approximately 100 mg of frozen stored heart tissue were blotted dry, quickly placed into liquid nitrogen and immediately ground to a fine powder; RNA was isolated, and analyzed, as described in chapter 2.2.

3.2.2.2 Reverse-transcription (RT)

First-strand complementary DNA was synthesized from 1 μg of total RNA by priming with gene-specific reverse primers, using Ready-To-Go RT-PCR beads (Amersham Pharmacia Biotech, Toronto). Each reaction contained 2.0 units of TaqDNA polymerase, 10 mM Tris-HCl, pH 9.0, 60 mM KCl, 1.5 mM $MgCl_2$, 200 μM of each dNTP, Moloney Murine Leukemia Virus (M-MuLV) reverse transcriptase, ribonuclease Inhibitor and stabilizers, and RNAse/DNAse-free BSA.

Gene-specific primers were synthesized from the sequences used by the Atlas macro array sets, which have been evaluated for their specificity（Table 3-1).

3.2.2.3 Housekeeping genes

GAPDH, β-actin, and ribosomal protein S29 were chosen as the housekeeping genes for this experiment. The housekeeping gene primer sequences and annealing temperatures are shown in Table 3-1.

Table 3-1: Primer used for Q-PCR

Gene Name	Annealing Temperature	Base pair	Primer sequence
H-FABP	59.2	288	(forward)ACACTGGACGGAGGCAAACTGGTC
			(reverse)AGGCTGGTGTCCCATATCTCCAGG
ACBP	57.6	211	(forward)ATCCAGGTCACCTCGCCAGTATGT
			(reverse)CCTTTCAGCTTGTTCCACGAGTCC
CPT	57.9	206	(forward)GGAAACACCGTTCACGCCATGATC
			(reverse)AAGCGACCTTTGTGGTAGACAGCC
MCAD	56.6	216	(forward)TCCGGAGAGTTGTGGTGGTCTTGG
			(reverse)GGTTCTGTCACGCAGTAGGCACAC
LCAD	57.6	230	(forward)CAAATGACATTCTTCGACTGTTTGTGG
			(reverse)GACTCAACTCTGGGTGGACAATTCC
VLCAD	57.0	201	(forward)CAAATGACATTCTTCGACTGTTTGTGG
			(reverse)GACTCAACTCTGGGTGGACAATTCC
ACS	54.9	198	(forward)GAAATGCCATGCTGGACTTGTGCAC
			(reverse)TTAACACCCACCTTATTGGTTGAAGTC
S29	57.9	236	(forward)TGAAGGCAAGATGGGTCACCAGCAGC
			(reverse)CAGGGTAGACAGTTGGTTTCATTGGG
GAPDH	57.6	286	(forward)TGTCAACGGATTTGGCCGTATTGGC
			(reverse)GAAGACGCCAGTAGACTCCACGAC
Actin	55.4	285	(forward)CCCTCTGAACCCTAAGGCCAACCG
			(reverse)GTGGTGGTGAAGCTGTAGCCACGC

3.2.3 Real time PCR

Real-time PCR was carried out in a Rotor-Gene 2000 thermocycler equipped with Rotor Gene 2000/3000 Real-time Amplification software version 4.6 (Corbett Research, Mortlake, Australia). The reaction volume was 25 µl.

3.2.3.1 Optimization of Q-PCR

Four factors needed to be optimized: SYBR Green I (SG) concentration, annealing temperature and time, the primer concentrations, and the $MgCl_2$ concentration.

3.2.3.1.1 SYBR Green I concentration optimization

Since SYBR Green I intercalates between the complementary strands of double stranded DNA, excessively high SYBR Green I concentrations can lead to an inhibition of the PCR reaction. However, if the SYBR Green I concentration is too low, the amplicon may not be labelled sufficiently. The optimal SG concentration therefore has to be a compromise between these two effects.

To obtain an optimal SG concentration, a dilution series containing 3 different dilutions of SG 1:50,000, 1:100,000 and 1: 500,000 were performed. From the results, it was concluded that 1:50,000 was the optimal choice.

3.2.3.1.2 Temperature and times

Three important parameters of the PCR-reaction are the denaturation, annealing, and extension temperatures. For the denaturation temperature, we used 95 °C, and the extension temperature is generally set at 72 °C. The optimal annealing temperature, however, is specific for each gene fragment. We determined the optimal annealing temperature for each PCR reaction with the Oligo-4-use software program, as shown in table 3-1.

A three-step experimental run protocol was used:

(1) Denaturation (5 min at 95 °C),

(2) Amplification and quantification, repeated 40 times (30 s at 95 °C; 20 s optimal annealing temperature for each gene with a single fluorescence measurement), 60 s at 72 °C

(3) Melting curve (60 °C to 99 °C with a heating rate of 0.1°C per second and a continuous fluorescence measurement)

3.2.3.1.3 Primer concentration

It is suggested that the primer concentration should be between 50 nM and 300 nM. The optimal primer concentration for a given reaction with a DNA template should result in a low Ct-value (threshold cycle) with a high increase in fluorescence (5 to 50 times), whereas the same reaction without DNA (no template control, NTC) should have a high Ct-value. High Ct-value of NTC is due to the formation of primer dimers or non-specific product. Two primer concentrations were tested, 50 nM and 100 nM. For the 100 nM primer concentration, primer dimers were observed in the melting curve, while the 50 nM concentration showed good results (data not shown); therefore, 50 nM was used in all subsequent experiments.

3.2.3.1.4 $MgCl_2$ concentration

Reducing the amount of $MgCl_2$ in the reaction can get more specific product. Several aspects of the amplification are affected by $MgCl_2$ concentration in a reaction. These include DNA polymerase activity, which can affect specificity. The dNTP and templates bind magnesium and reduce the amount of free magnesium available for enzyme activity. However, for each primer pair and template, optimal magnesium concentrations vary. Greater yields of amplification product can be achieved with higher concentration of free magnesium, but this can also increase non-specific amplification. In my experiments, 1.5 mM $MgCl_2$

generally showed good qRT-PCR results, i.e., good levels of specific amplification without formation of non-specific by-products (data not shown).

3.2.3.2 Standard curve

For each gene fragment, serial dilutions of the PCR products to yield DNA concentrations between 1 pg and 100 ng, to find the optimal concentration range for quantitative amplification. Based on these preliminary results, 3 concentrations were chosen for each gene to make a standard curve.

3.2.3.3 Real time PCR reaction

Total RNA (1 µg) was used as the template for reverse transcription by Ready-To-Go RT-PCR beads. The reaction was carried out in the thermocycler at 25 °C for 5 mins, 95 °C for 5 min, and 45 °C for 45 mins. After completion of the RT procedure, the cDNA was diluted to the optimized cDNA concentration range for real-time PCR with standard and NTC.

3.2.3.4 Intra-assay precision test

To confirm the precision of real-time PCR, the intra-assay precision was determined in 2 repeats within one run. I used H-FABP to do duplicate test (primers: R1 and R4, conditions: denaturation for 4 min at 95 °C, 40 cycles of 30 seconds at 95 °C, 30 seconds at 54 °C, 30 seconds at 72 °C. The experimental results showed good reproducibility (Fig. 3-1).

No.	Colour	Name	Type	Given Conc.	Calculated	CV	Ct
1		1-1	Standard	1.0000	0.7057	29.43%	3.23
2		1-2	Standard	1.0000	0.7381	26.19%	3.17
3		2-1	Standard	0.1000	0.1697	69.68%	5.14
4		2-2	Standard	0.1000	0.1006	0.64%	5.84
5		3-1	Standard	0.0100	0.0167	66.60%	8.25
6		3-2	Standard	0.0100	0.0100	0.30%	8.93
7		4-1	Standard	0.0010	0.0007	26.93%	12.44
8		4-2	Standard	0.0010	0.0009	7.92%	12.13

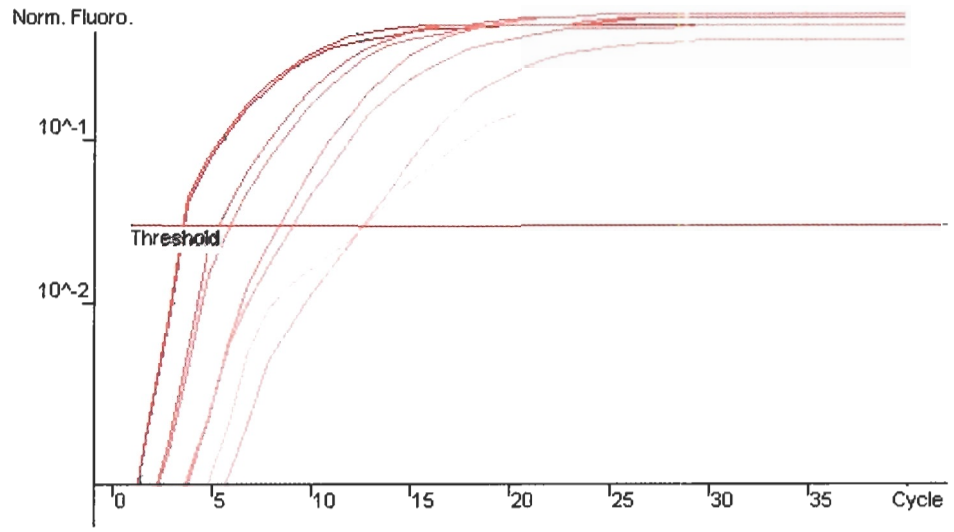

Fig. 3-1: Duplicated test

Duplicated test: 1-1, 1-2 is parallel test, which show standard deviation is 0.03. 2-1, 2-2 are parallel test, which show standard deviation is 0.35, 3-1, 3-2 are parallel test, which show standard deviation is 0.34; 4-1, 4-2 are parallel, which show standard deviation is 0.15.

3.2.3.5 Relative quantitation

There are two different ways of quantitation: absolute and relative. Absolute quantitation uses a known input amount mRNA (copy numbers) which results in an absolute output amount of copy numbers. In our experiments, the absolute numbers present in the tissue cannot be determined, as multiple losses due to the separation steps and degradation may occur. However, it is possible to obtain relative quantitative ratio by comparing diabetic rat heart sample with normal rat heart sample. This relative quantitation only determines levels relative to the standard, given as a ratio. To obtain differences between normal and diabetic animals, each sample thus has to be analyzed twice: first to compare control with diabetic sample housekeeping gene, and then a target gene. Standard curves have to be run to obtain amplification efficiency for both the housekeeping genes and the specific genes. The relative ratio between specific templates in the diabetic sample and control sample is then calculated by dividing the changes of the gene in question by housekeeping gene changes, using the standard curves to get the efficiency and adjust its values.

3.2.3.5.1 Relative Expression Software Tool (REST)

Today, several mathematical algorithms have been developed to compute a relative expression ratio, The Relative Expression Software Tool (REST)

(Michael et al., 2002) is good software to analyse real time PCR results. REST compares two groups, for reference and up to four target genes. The mathematical model used is based on the PCR efficiencies and the mean crossing point deviation between sample and control group. The real-time PCR efficiencies are calculated from the slope of standard curve, according to the established equation $E = 10^{[-1/slope]}$ (E in the range from 1 to 2). Equation 1 shows the mathematical model, which includes an efficiency correction for real-time PCR efficiency of the individual transcripts. In my data analysis, I use equation 1 to calculate the relative expression ratio of control and diabetic sample for each specific gene I chosen.

It calculates the relative expression ratio on the basis of the PCR efficiency (E) and crossing point deviation (△CP) for each specific gene of diabetic sample versus control (△CP (control - sample)).

$$R = \frac{(E_{target})^{\Delta CPtarget\ (control - sample)}}{(E_{ref})^{\Delta CPref\ (control - sample)}}$$

Equation 1: E is PCR efficiency, △CP is cross point deviation.

In mathematical models, the specific gene expression is normalized with respect to housekeeping gene expression. As stated above, I choose three housekeeping genes for normalization, glyceraldehyde-3-phosphate dehydrogenase (GAPDH), β-actin, and S29 ribosomal RNA.

3.3 Results

3.3.1 Quantitation standard curves

Standard curves for the housekeeping genes S29 ribosomal subunit, GAPDH, and β-actin were generated from serial dilutions of cDNAs (1 pg, 10 pg, 100 pg, 1 ng, 10 ng, 100 ng) made from PCR products of the specific gene fragments. In all cases, the linear phase was between 8 and 18 cycles, allowing the quantification of target concentrations in the pico- to nanogram range. The standard curves for GAPDH and S29 RNA are shown in Fig. 3.2 and 3.3, respectively. In all cases, melting curves yielded a single, sharp peak, demonstrating that a single homogeneous amplification product is detected.

Similar standard curves were generated for each of the target genes investigated (FABP, ACS, CPT-I, ACBP, LCAD, and VLCAD). The results for two of these (FABP and ACBP) are shown in Fig. 3.4 and 3.5. Similar to those two genes, template concentrations for linear amplification of the other target genes were also in the pico- and nanogram range, and the amplicons had well-defined melting curves.

Subsequently, cDNA from diabetic and control rat heart was used as template for each of these targets, and their relative values measured by real time PCR. A representative result is shown for the housekeeping gene β-actin (Fig. 3-6).

3.3.2 Target gene changes

The data from the real time experiments were normalized against each of the three housekeeping genes, using data analysis by the REST software. The data are summarized in Table 3-2, 3-3 and 3-4. Each Ct value shown is the mean of several independent experiments. In all cases, ACS mRNA was drastically reduced in diabetic tissue, while FABP, ACBP, and LCAD stayed at similiar levels. CPT, MCAD, and VLCAD appear to be increased. Because normalization against the different housekeeping genes resulted in similar, but not identical results, the overall changes were averaged. Table 3-5 compares the changes observed in diabetic animals with the three genes used for normalization, and shows the mean values as well as the standard deviation as a measure for the variations. These data demonstrate that each of the housekeeping genes gives similar results, with deviations between 8 and 11 % only.

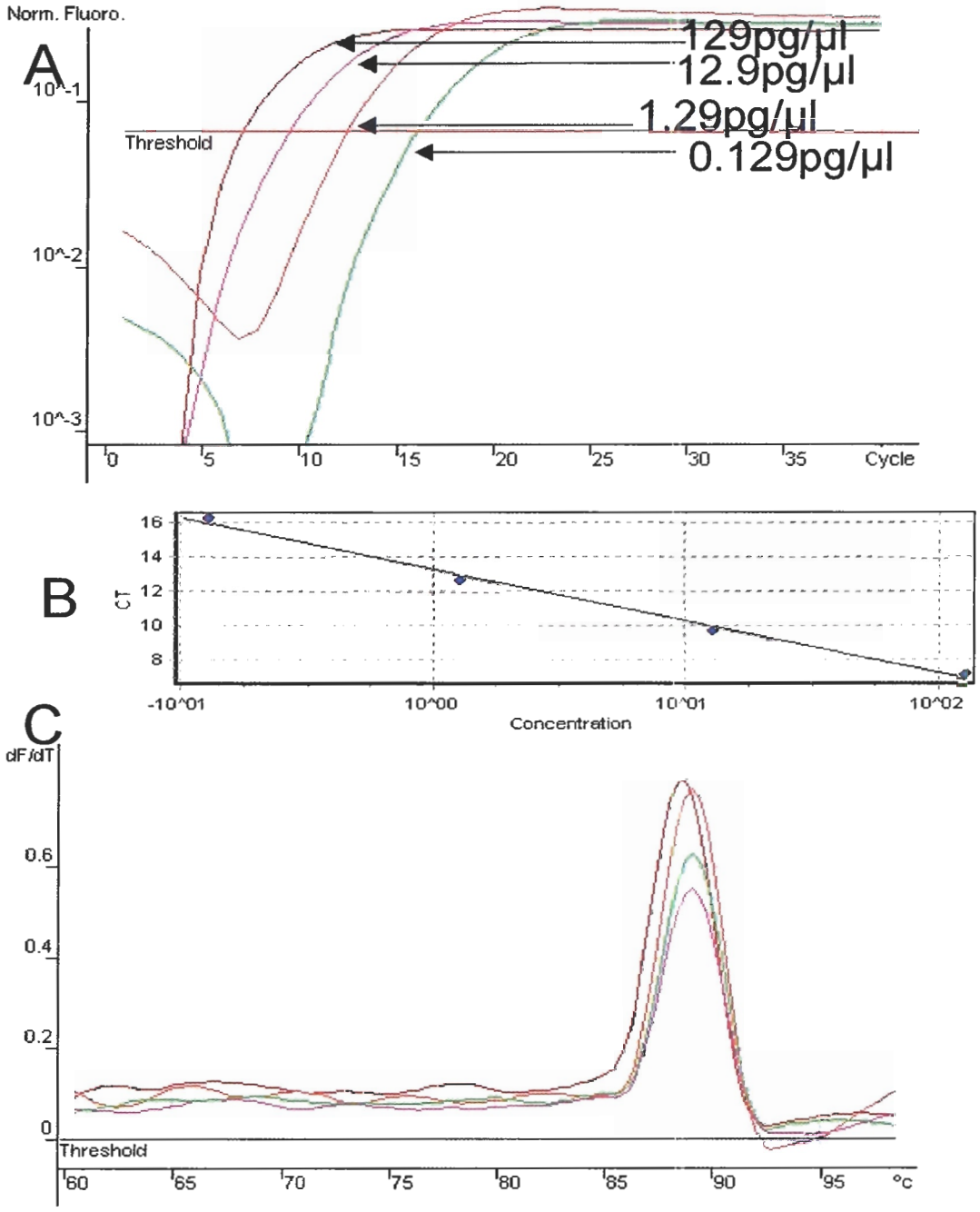

Fig. 3-2: Quantitative real time PCR for GAPDH

A: Standard curve with varying concentrations of template cDNA, as indicated.

B. Standard curve constructed from the data shown in panel A.

C: Melting curves for the PCR products, as shown in panel A.

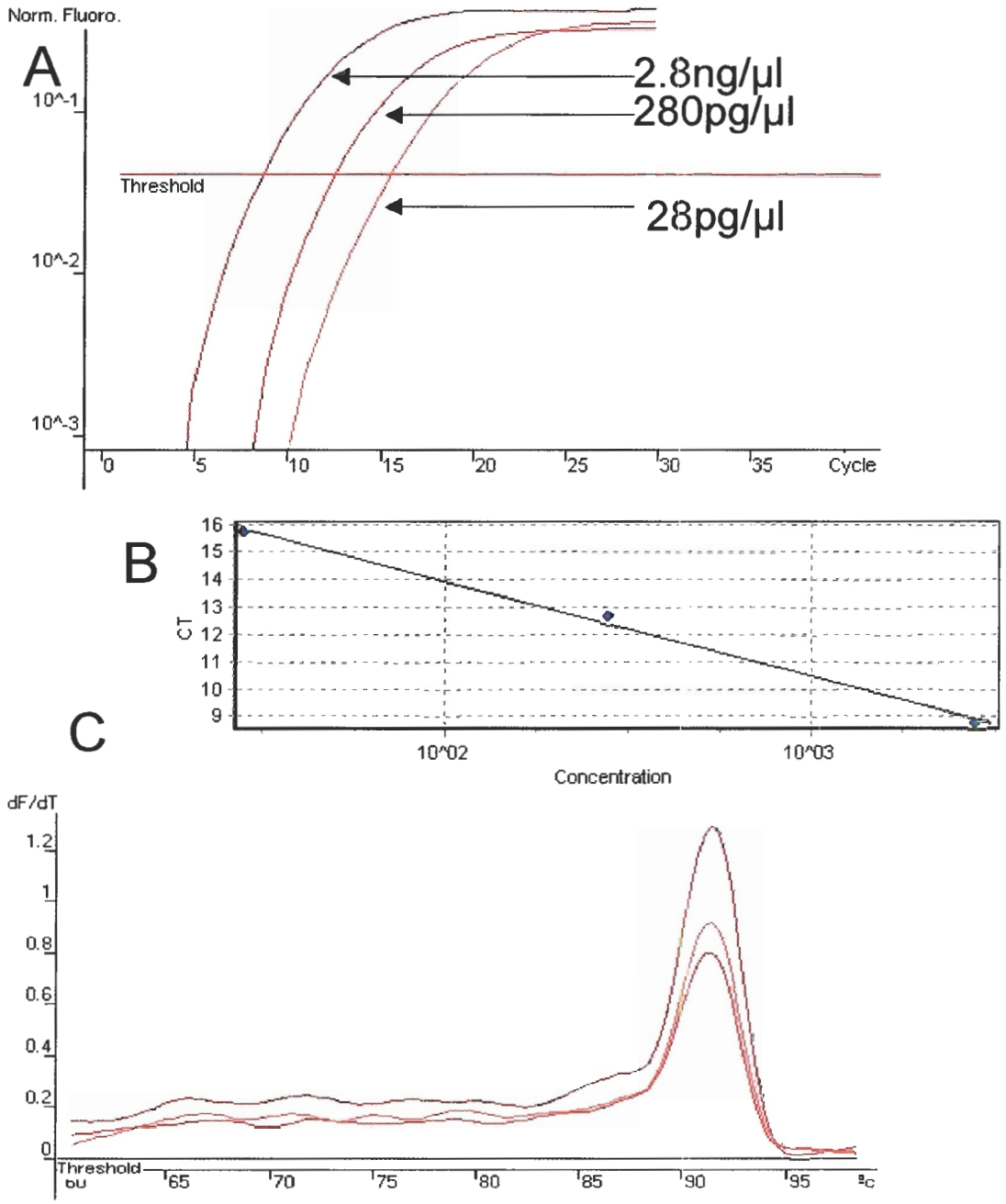

Fig. 3-3: Quantitative real time PCR for S29

A: Standard curve with varying concentrations of template cDNA, as indicated.

B. Standard curve constructed from the data shown in panel A.

C: Melting curves for the PCR products, as shown in panel A.

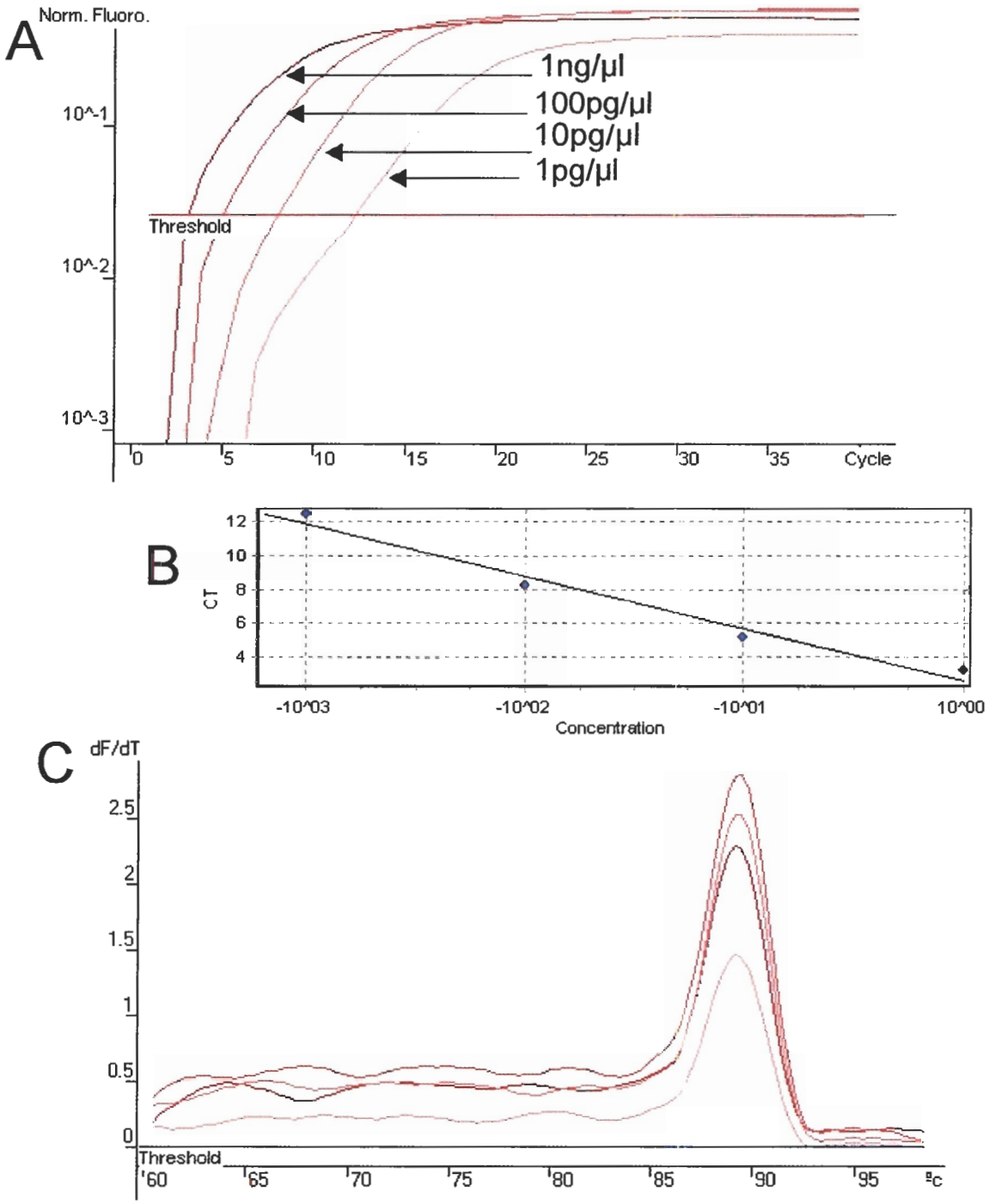

Fig. 3-4: Quantitative real time PCR for FABP

A: Standard curve with varying concentrations of template cDNA, as indicated.

B. Standard curve constructed from the data shown in panel A.

C: Melting curves for the PCR products, as shown in panel A.

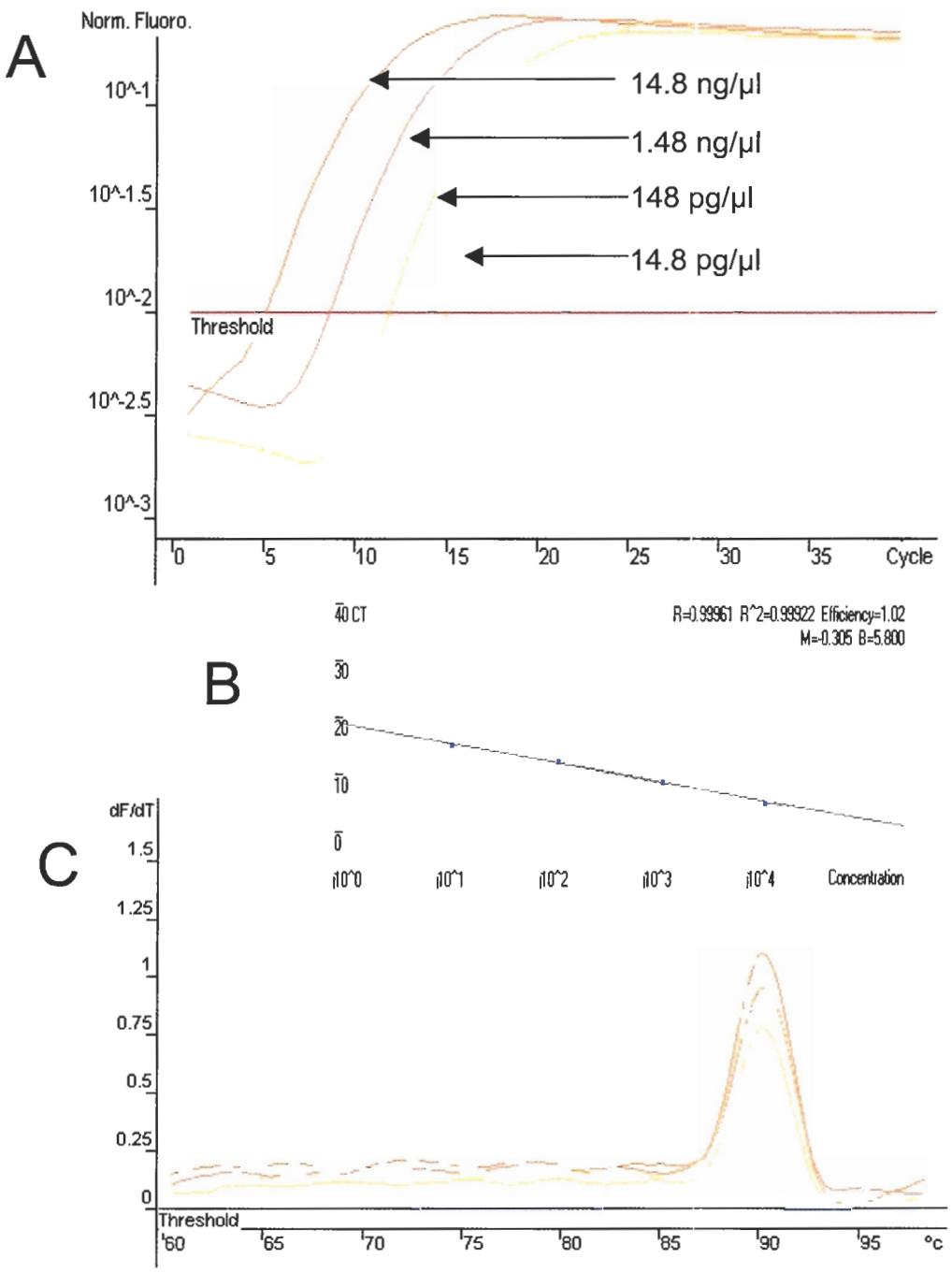

Fig. 3-5: Quantitative real time PCR for ACBP

A: Standard curve with varying concentrations of template cDNA, as indicated.

B. Standard curve constructed from the data shown in panel A.

C: Melting curves for the PCR products, as shown in panel A.

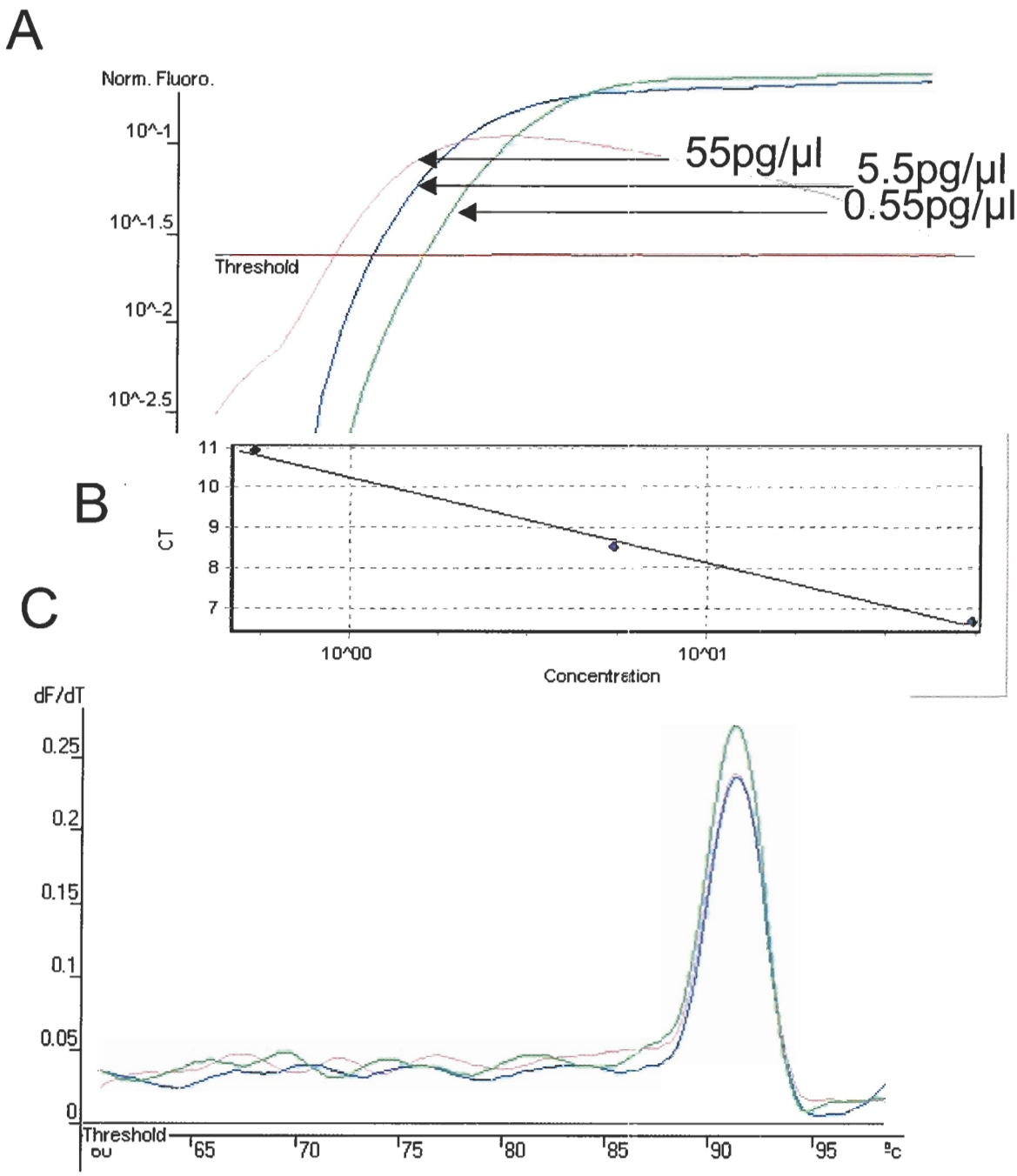

Fig. 3-6: Quantitative real time PCR for Actin (Control and diabetic sample)

A: Standard curve with varying concentrations of template cDNA, as indicated.

B. Standard curve constructed from the data shown in panel A.

C: Melting curves for the PCR products, as shown in panel A.

Table 3-2: Gene expression changes relative to S29 mRNA

Gene Name	FABP	ACS	CPT	ACBP	MCAD	LCAD	VLCAD
$Efficiency_{(target)}$	2.00	2.00	1.74	2.00	2.00	2.00	1.91
$Mean_{control}$	12.73	19.92	18.40	17.11	18.53	16.84	18.07
$Mean_{Diabetic}$	12.58	21.24	17.80	16.92	18.07	16.78	17.41
$E_{(target)}^{\Delta CP}$	1.171	0.401	1.392	1.137	1.582	1.039	1.536
Ratio (R)	0.91	0.31	1.08	0.88	1.23	0.81	1.19

Efficiency = 1.82, $E_{(S29)}^{\Delta CP}$=1.288; R= ratio diabetic to control sample. n=2-6.

Table 3-3: Gene expression changes relative to beta-actin mRNA

Gene Name	FABP	ACS	CPT	ACBP	MCAD	LCAD	VLCAD
$Efficiency_{(target)}$	2.00	2.00	1.74	2.00	2.00	2.00	1.91
$Mean_{control}$	12.73	19.92	18.40	17.11	18.53	16.84	18.07
$Mean_{Diabetic}$	12.58	21.24	17.80	16.92	18.07	16.78	17.41
$E_{(target)}^{\Delta CP}$	1.171	0.401	1.392	1.137	1.582	1.039	1.536
Ratio (R)	0.94	0.34	1.16	0.94	1.27	0.86	1.27

Efficiency = 2.00, $E_{(actin)}^{\Delta CP}$=1.177; R= ratio diabetic to control sample. n=2-6.

Table 3-4: Gene expression changes relative to GAPDH mRNA

Gene Name	FABP	ACS	CPT	ACBP	MCAD	LCAD	VLCAD
$Efficiency_{(target)}$	2.00	2.00	1.74	2.00	2.00	2.00	1.91
$Mean_{control}$	12.73	19.92	18.40	17.11	18.53	16.84	18.07
$Mean_{Diabetic}$	12.58	21.24	17.80	16.92	18.07	16.78	17.41
$E_{(target)}^{\Delta CP}$	1.171	0.401	1.392	1.137	1.582	1.039	1.536
Ratio (R)	1.09	0.37	1.31	1.06	1.48	0.97	1.43

Efficiency = 2.00, $E_{(GAPDH)}^{\Delta CP}$=1.072; R= ratio diabetic to control sample. n=2-6.

Table 3-5: Gene expression changes normalized to all housekeeping genes

Gene	FABP	ACS	CPT	ACBP	MCAD	LCAD	VLCAD
GAPDH	1.09	0.37	1.31	1.06	1.48	0.97	1.43
β -actin	0.94	0.34	1.14	0.93	1.27	0.85	1.25
S29	0.91	0.31	1.08	0.88	1.23	0.81	1.19
Average	0.98	0.34	1.18	0.96	1.33	0.88	1.29
± S.D	± 0.11	± 0.03	± 0.13	± 0.10	± 0.15	± 0.07	± 0.14
	(±1.2%)	(±8.8 %)	(±11.0 %)	(±10.4 %)	(±11.2 %)	(±8.0 %)	(±10.9 %)

3.4 Discussion

qRT-PCR is a sensitive method to detect and quantity gene expression levels. It is easy to perform and it is possible to get relatively high throughput, with high sensitivity and reliable specificity. However, it is a very complex technique with various substantial problems associated with its sensitivity, reproducibility and specificity. Therefore, there are still many practical problems. Most critical is the normalization method, choosing constant genes in different samples. If we cannot identify constant genes in different samples, it is not easy to obtain unambiguous data even though all technical problems may be minimized. Therefore, the identification of valid housekeeping genes for data normalization is the most stubborn of problems. At present, no one method is ideal to measure gene expression changes.

Today, total RNA, rRNA or housekeeping genes are used for normalization in most quantitative expression experiments. All quantitative methods assume that the RNA targets are reverse-transcribed and subsequently amplified with similar efficiency. A main problem is the lack of an internal control for the reverse transcription reaction. The samples might contain inhibitor that significantly reduces the efficiency of the RT-PCR reaction which results in inaccurate quantification.

Normalization against total RNA is problematic and unreliable. One study showed total RNA levels remaining constant during serum-stimulation of cultured cells (Schmittgen and Zakrajsek, 2000) while Bustin et al. (2000) reported that normalization to total cellular RNA is the least reliable method. The reason is because we know little about the total RNA content per cell of different tissues and the variation between individuals or, in the research presented here, between normal and diabetic tissue.

Ribosomal RNA has been used as a normalization method (Bhatia et al., 1994, Zhong and Simons, 1999), but it has the same problem as total RNA because the abundance of rRNA vastly exceeds any other transcript. Moreover, Solanas et al. (2001) have suggested that it is unreliable for normalization due to variations in expression, transcription by a different RNA polymerase, and possible imbalances between different samples.

Housekeeping genes are present in all nucleated cell types since, by definition, they are necessary for basic cell survival. The mRNA synthesis of these genes is considered to be stable in various tissues, even under varying experimental treatments. However, it is very hard to predict which housekeeping gene might be useful under specific circumstances; indeed, the mRNA levels of housekeeping genes are not always constant, and may vary to different degrees. Thus, we can never rely on a single housekeeping gene alone for normalization.

Among the housekeeping genes most commonly used for normalization are ß-actin, GAPDH, cyclophilin, 18S rRNA, 28S rRNA, ribosomal protein S29, phosphoglycerokinase, ß-2-microglobulin, ß-glucronidase, hypoxanthine ribosyl transferase, transferrin receptor and others. Many papers have shown that housekeeping genes or internal controls may be influenced by assay conditions (Baset al., 2004, Joeri et al., 2004, Radonic et al., 2004, Vandesompele et al., 2002). When choosing housekeeping genes for this study, it was important to consider the effect of diabetic metabolism on housekeeping gene expression. To date, there are no reports that the expression of these housekeeping genes is stable in diabetic rat heart. Therefore, I chose three different housekeeping genes for the normalization, GAPDH, ß-actin, and ribosomal protein S29. These three standards represent three different functions: GAPDH is a protein involved in basic energy metabolism, ß-actin is a structural protein, and S29 is required for protein synthesis. The data normalized against the three housekeeping gene are summarized in table 3-5. Since the data are consistent for all of these genes, it is likely that the genes are indeed not changing during treatment. Moreover, the expression of these genes appeared largely constant in the macroarray experiments (chapter 2), and hence they were also used to normalize the macro array experiments. The real time PCR experiments summarized in Table 3-5 confirm this finding.

From real time PCR experiments, CPT (1.18x), MCAD (1.33x) and VLCAD (1.29x) appear to be slightly up-regulated, while FABP (0.98x) and ACBP (0.96x) remain unchanged in diabetic rat hearts. These results are mostly similar to the results from the macroarray experiments. In these, we found many genes down-regulated in diabetic rat hearts, including several that are related to energy metabolism. In contrast, the mRNAs for most genes involved in fatty acid transport and metabolism are not going down: they either remain constant or are increased. This indicates that the entire lipid metabolism complex is more active in diabetic rat heart, compensating for the lack of glucose as reliable energy source. Genes found to be up-regulated in the array experiments include CPT (3.04x), MCAD (1.15x), LCAD (2.45x), VLCAD (30x) and ACBP (31x). The very high values for the latter two genes seen in the macroarray are, however, most likely incorrect; the spots seen for control animals are just slightly above background, and therefore may under-represent the actual amount of mRNA. The ACS gene spot on the macroarrays was very strong as well, but not saturated in the control animals. However, there is a big difference between real time PCR and macroarray for this gene: real time PCR shows 0.34-fold down-regulation, while the spots on macroarray show a nearly 1.93-fold up-regulation. At present, we cannot explain this discrepancy; it may be possible that in the array other, cross-hybridizing messages were also detected. Generally, the real time PCR results appear far more reproducible and quantitative. Although the direction of changes is often similar between the two techniques, there was little consistency in the numeric values between the macroarrays and real time PCR.

For many highly expressed genes, including FABP, the macroarray results are misleading because saturated spots are seen in both control and diabetic animals. Through normalization the value for diabetic animals will be increased, thus suggesting up-regulation when it is in fact impossible to decide whether increases or decreases in expression took place. Because of these and the other limitations in the macroarray experiments, as discussed above and in Chapters 2 and 3, we conclude that the macroarray data are probably less reliable, and that the values of the real-time PCR experiments more accurately reflect the changes in mRNA.

CHAPTER 4: GENERAL DISCUSSION

In this project, we investigated gene changes in the diabetic heart by macroarray and real time PCR. DNA macroarray allows simultaneous analysis of expression of thousands of genes. By DNA macroarray, we have detected gene expression changes in diabetic rat hearts. These genes include a number of genes involved in lipid metabolism, in carbohydrate metabolism, and in ion channel transport and they are discussed in more detail below.

Lipid metabolism:

Diabetes is a disorder of fatty acid metabolism while it is also a disorder of glucose metabolism (McGarry, 1992). In response to elevations in fatty acid levels, mammalian tissues increase the expression of various proteins involved in fatty acid utilization (Kersten, 1999). In the array experiment, the expression of 130 genes was down-regulated in the diabetic rat heart, reflecting the decreased metabolism of these animals. In contrast, the expression of fatty acid metabolism related genes (fatty acid binding protein, acyl-CoA dehydrogenase, and CPT) remain largely constant, while others (long chain acyl-CoA synthetase 2, acyl-CoA oxidase, acyl-CoA synthetase, acyl-CoA binding protein, mitochondrial

muscle carnitine O-palmitoyl transferase, medium chain fatty acid acyl-CoA dehydrogenase, long chain fatty acid acyl-CoA dehydrogenase, very long chain fatty acid acyl-CoA dehydrogenase) are up-regulated. Apolipoprotein D, adipocyte fatty acid binding protein (A-FABP), and mitogen-activated protein kinase 5 (MAP kinase kinase 5) appear to be down regulated. Some of these results are consistent with previously published data, namely medium chain acetyl-CoA dehydrogenase (reported up in 1.38 fold, Vijay et al., 2002) carnitine acetyltransferase (reported up 1.65 fold Vijay et al., 2002), and Acyl-CoA thioesterase 1 (reported up 3.71 fold, Vijay et al., 2002). All these changes indicate the entire lipid metabolism complex is more active in diabetic rat heart, compensating for the lack of glucose as reliable energy source. At the same time, the real time PCR experiment show that MCAD is up regulated 1.33 fold, which is consistent with the published data (1.38). However, due to the experimental limitation we discussed before, some of data show variation between macroarrays and real time PCR, which are not easily understood.

Ion channel regulation:

Because heart muscle from diabetic animals exhibits a slow rate of relaxation, the sarcoplasmic reticulum Ca^{2+} ATPase (SERCA) 2 has been considered a major site for contractile dysfunction (Rupp et al., 1994). SERCA2 is regulated transcriptionally by the metabolic status of the cardiomyocyte. Both SERCA2a mRNA, the major splice variant in the heart, and its enzymatic activity decrease in

response to pressure overload and diabetes. It has been shown that abnormalities of intracellular Ca^{2+} metabolism cause cardiac dysfunction in STZ-induced diabetic rats heart (Rupp et al., 1994). Defects in the sarcolemmal Ca^{2+} pump and Na- Ca^{2+} exchanger, decreased L-type Ca^{2+} current and dysfunction of the sarcoplasmic reticulum were emerging in the STZ diabetic heart, suggesting a possible pathogeneses of impaired Ca^{2+} flow in the diabetic heart. In addition, insulin-deficient type I diabetes is associated with early down regulation of the expression of key cardiac K^+ channel genes that could account for the depression of cardiac K^+ currents (Hector et al., 2003). These represent the main electrophysiological abnormality in diabetic cardiomyopathy, which is known to enhance the arrhythmogenicity of the diabetic heart.

From my experiments, it appears that sodium channel SHRSPHD, gamma subunit, ATP-sensitive inward rectifier potassium sunfamily 8 (KCNJ8) and the voltage-gated K^+ channel protein RK5 are down-regulated. Other ion-channel proteins that appear to be down regulated include dihydropyridine-sensitive L-type calcium channel alpha 2, calcium channel 1 potassium channel Kir 6.2 (ATP-sensitive, sodium channel β1 subunit, sodium/potassium-transporting ATPase isoform 2 β polypeptide 2(Na+/K+ ATPase 2 β 2), Na+/K+ ATPase alpha, Na, K ATPase β 3 subunit, hydrogen-potassium ATPase.

While it appears that many calcium and potassium channel regulation proteins are down-regulated in diabetes, these alterations have not been verified by real-

time PCR. If confirmed, these changes have clear physiological implications for the diabetic heart, and it would be important to study the mechanism by which these genes are down-regulated.

From the macroarray experiments, we also found that other genes appear to be down-regulated: Inducible nitric oxide synthase (iNOS), fibroblast growth factor 5 (FGF5), Insulin-like growth factor binding protein 6 (IGFBP6) and 1 (IGFBP1), NADPH-cytochrome P450 reductase (CPR), $NADP^+$ alcohol dehydrogenase, protein kinase C delta type (PKC-delta), gamma (PKC-gamma), zeta (PKC-zeta) and insulin-like growth factor 2 (IGF2). The latter mRNA has previously been demonstrated to be reduced to 70 % in diabetic hearts (Leaman et al., 1990, Bornfeldt et al., 1992)

An overview of gene expression profiles in diabetic hearts is an efficient way to uncover clues to specific molecular derangements that lead to the pathogenesis of this devastating disease. Recognition of pathogenomic alterations in gene expression might provide a basis for improved diagnosis and molecular classification of diabetic heart and therefore allow selection of the most appropriate therapeutic strategies. While microarray experiments clearly have tremendous potential, it is important to recognize the limitations of these techniques. For most genes, the direction of gene expression changes was similar between macroarray and real-time PCR experiments, but the numerical increase or decrease significantly differed between the two methods. In

conclusion, macroarray analysis is a valid survey technique to identify potential gene expression changes in the heart of diabetic rats, but quantitative analysis requires verification by real-time PCR.

REFERENCE LIST

Aerts JL, Gonzales MI, and Topalian SL (2004) Selection of appropriate control genes to assess expression of tumor antigens using real-time RT-PCR. *Biotechniques* **36**, 84-91.

Afzal N, Ganguly PK, Dhalla KS, Pierce GN, Singal PK, and Dhalla NS (1988) Beneficial effects of verapamil in diabetic cardiomyopathy. *Diabetes* **37**, 936-924.

American Diabetes Association. (2002) Facts and Figures: Direct and Indirect Costs of Diabetes. http://www.diabetes.org/main/info/facts/impact/default2.jsp. Accessed June 19.

Andries J, Gilde AJ, Karin AJM, and Van der Lee KAJM (2003) Peroxisome proliferators-activated receptor (PPAR) α and PPARβ/δ, but not PPARγ, modulate the expression of genes involved in cardiac lipid metabolism. *Circ. Res.* **92**, 518-524.

Bas A, Forsberg G, Hammarstrom S, and Hammarstrom ML (2004) Utility of the housekeeping genes 18S rRNA, β-Actin and glyceraldehydes-3-phosphate-dehydrogenase for normalization in real-time quantitative reverse transcriptase-

polymerase chain reaction analysis of gene expression in human T lymphocytes. *Scan. J. Immun.* **59**, 566-573.

Bell DS (1995) Diabetic cardiomyopathy: A unique entity or a complication of coronary artery disease. *Diabetes Care* **18**, 708-714.

Bhatia P, Taylor WR, Greenberg AH, and Wright JA (1994) Comparison of glyceraldehyde-3-phosphate dehydrogenase and 28S-ribosomal RNA gene expression as RNA loading controls for northern blot analysis of cell lines of varying malignant potential. *Anal Biochem.* **216**, 223-226.

Bierman E (1992) Atherogenesis in diabetes. *Atheroscl. Thromb.* **12**, 647-656.

Bornfeldt KE, Skottner A, and Arnqvist HJ (1992) In-vivo regulation of messenger RNA encoding insulin-like growth factor-I (IGF-I) and its receptor by diabetes, insulin and IGF-I in rat muscle. *Endocrinology* ,**135**, 203-211.

Breyer J (1998) Diabetic Nephropathy. In: Greenberg A (ed) Primer on kidney diseases . *Academic Press, New York*, pp 215-220.

Brinkmann JF, Abumrad NA, Ibrahimi A, van der Vusse GJ, and Glatz JF (2002) New insights into long-chain fatty acid uptake by heart muscle: a crucial role for fatty acid translocase/CD36. *Biochem. J.* **367,** 561-570.

Bustin SA (2000) Absolute quantification of mRNA using real-time reverse transcription polymerase chain reaction assays. *J. Mol. Endocrinol.* **25**,169-93.

Choi KH, Kang SW, Lee HY, and Han DS (1996) The effects of high glucose concentration on angiotensin II or transforming growth factor-β-induced DNA synthesis, hypertrophy and collgen synthesis in cultured rat mesangial cells. *Yonsei Med. J.* **37**, 302-311.

Chiu KC, Chuang LM, Chu A, and Yoon C (2001) Fatty acid binding protein 2 and insulin resistance. *Eur. J. Clin. Invest.* **31**, 521-527.

Condon C, and Putzer H (2002) The phylogenetic distribution of bacterial ribonucleases. *Nucl. Acids Res.* **30**, 5339-5346.

Derubertis FR, and Craven PA (1994) Activation of protein kinase C in glomerular cells in diabetes: mechanisms and potential links to the pathogenesis of diabetic glomerulopathy. *Diabetes* **43**, 1-8.

Diabetes control and complications trial research group (1993) The effect of intensive therapy of diabetes mellitus in the development and progression of long term complications of IDDM. *N. Engl. J. Med.* **329**, 977-986.

Eisenberg S, and Levy RI (1976) Lipoprotein metabolism, *Adv. Lipid Res.* **13**, 1-23.

Emmert-Buck MR, Bonner RF, Smith PD, Chuaqui RF, Zhuang Z, Goldstein SR, Weiss RA, and Liotta LA (1996) Laser capture microdissection. *Science,* **274**, 998-1001.

Engels W, van Bilsen M, Wolffenbuttel BH, van der Vusse GJ, and Glatz JF (1999) Cytochrome P450, peroxisome proliferation, and cytoplasmic fatty acid-binding protein content in liver, heart and kidney of the diabetic rat. *Mol. cell Biochem.* **192**, 53-61.

Faust IM (1980) Nutrition and the fat cell, *Int. J. Obesity.* **4**, 314-330.

Garvey WT, Hardin D, Juhaszova M, and Dominguez JH (1993) Effects of diabetes on myocardial glucose transport system in rats: implications from diabetic cardiomyopathy. *Am. J. Physiol.* **264**, H837-844.

Garvey WT, Maianu L, Hueckstead TP, Birnaum MJ, Molina JM, and Ciaraldi TP (1991) Pretranslational suppression of GLUT4 glucose transporters causes insulin resistance in type II diabetes. *J. Clin. Invest.* 87: 1072-1081.

Giles TD, Ouyang J, Kerut EK, Given MB, Allen GE, and McIlwain EF (1998) Changes in protein kinase C in early cardiomyopathy and in gracilis muscle in the BB/W or diabetic rat. *Am. J. Physiol.* **274**, 295-307

.

Glatz JFC (1994) Rat heart fatty acid-binding protein content is increased in experimental diabetes. *Biochem. Biophys. Res. Commun.* **199**, 639-646.

Golfman L, Dixon IM, Takeda N, Lukas A, Dakshinamurti K, and Dhalla NS (1998) Cardiac sarcolemmal Na(+)-Ca2+ exchange and Na(+)-K+ ATPase activities and gene expression in alloxan-induced diabetes in rats. *Mol. Cell Biochem.* **188**, 91-101.

Goldberg IJ (2001) Clinical review 124: Diabetic dyslipidemia: causes and consequences. *J. Clin. Endocrinol. Metab.* **86**, 965-71.

Haffner SM, Stern MP, Hazuda HP, Mitchell BD, Patterson JK (1990) Cardiovascular risk factors in confirmed prediabetic individuals. Does the clock for coronary heart disease start ticking before the onset of clinical diabetes? *J. Amer. Med. Association,* **263**, 2893-2898.

Han I, and Kudlow JE (1997) Reduced O-glycosylation of Sp1 is associated with increased proteasome susceptibility. *Mol Cell. Biol.* **17,** 1550-1558.

Handberg A, Vaag A, Vinte J, and Back-Nielsen H (1993) Decreased tyrosine kinase activity in partially purified insulin receptors from muscle of young non-obese first degree relatives of patients with Type 2 (non-insulin-dependent) diabetes mellitus. *Diabetologia* **36,** 668-674.

Haunerland NH (1994) Fatty acid binding protein in locust and mammalian muscle. Comparison of structure, function, and regulation. *Comp. Biochem. Physiol.* **109B**, 199-208.

Hidaka S, Kakuma T, Yoshimatsu H, Sakino H, Fukuchi S, and Sakata T (1999) Streptozotocin treatment upregulates uncoupling protein 3 expression in the rat heart. *Diabetes* **48,** 430-435.

Kahn HA and Hiller R. (1974) Blindness caused by diabetic retinopathy. *Am. J. Ophthalmol.* **78**, 58-67.

Kersten S, Seydoux J, Peters JM, Gonzalez FJ, Desvergne B, and Wahli W (1999) Peroxisome proliferators-activated receptor alpha mediates the adaptive response to fasting. *J. Clin. Invest.* **103,**1489-1498.

Kim SI, Han DC, Kohane IS, Kho AT, and Butte AJ (2003) Microarrays for an integrative genomics. 1st edit, 1. 1 vols, MIT Press, London.

Kuller LH, Velentgas P, Barzilay J, Beauchamp NJ, O'Leary DH, and Savage PJ (2000) Diabetes Mellitus Subclinical cardiovascular disease and risk of incident cardiovascular disease and all-cause mortality. *Arterioscler. Thromb. Vasc. Biol.* **20**, 823-829.

Leaman DW, Simmen FA, Ramsay TG, and White ME (1990) Insulin-like growth factor-I and –II messenger RNA expression in muscle, heart, and liver of streptozotocin-diabetic swine. *Endocrinology* **126**, 2850-2857.

Lee HB. (2000) Lovastatin inhibits transforming growth factor-β expression in diabetic rat glomeruli and cultured rat mesangial cells. *J. Am. Soc. Nephrol.* **11**, 80-87.

Lekanne-Deprez RH, Fijnvandraat AC, Ruijter JM, Moorman AF (2002) Sensitivity and accuracy of quantitative real-time polymerase chain reaction using SYBR green I depends on cDNA synthesis conditions. *Anal. Biochem.* **307**, 63-69.

Ling BN (1996) Regulation of mesangial chloride channels by insulin and glucose: role in diabetic nephropathy. *Clin. Exp. Pharmacol. Physiol.* **23**, 89-94.

Mario B, and David M (2004) Structure and Function of the Vessel Wall. *Diabetes Cardiovasc. Dis.* **51**, 3-18.

McGarry JD (1992) What if Minkowski had been ageusic? An alternative angle on diabetes. *Science* **258,** 766-770.

McGarry JD, and Dobbins RL (1999) Fatty acids, lipotoxicity and insulin secretion. *Diabetologia* **42**,128-138.

McNeill JH (1999) Experimental models of diabetes. *CRC Press*, 418-423.

Pfaffl MW, Horgan GW, and Dempfle L (2002) Relative expression software tool (REST©) for group-wise comparison and statistical analysis of relative expression results in real-time PCR. *Nucl. Acids Res.* **30**, 36-46

Montford I, and Perez-Tamayo R (1962) The muscle-collagen ration in normal and hypertrophic human hearts. *Lab Invest.* **11**, 463-470

Nair S, and Pitchumoni CS (1997) Diabetic ketoacidosis, hyperlipidemia, and acute pancreatitis: the enigmatic triangle. *Amer. J. Gastro.* **92**, 1560-1560.

Newgard CB, and McGarry JD (1995) Metabolic coupling factors in pancreatic β–cell signal transduction. *Annu. Rev. Biochem.* **64**, 6689-6719.

Plate KH (1992) Vascular endothelial growth factor is a potential tumour angiogenesis factor in human gliomas in vivo. *Nature* **359,** 845-848.

Pierce EA (1995) Vascular endothelial growth factor/vascular permeability factor expression in a mouse model of retinal neovascularization. *Proc. Natl. Acad. Sci.* USA **92**, 905-909.

Pierce GN, Ramjiawan B, Dhalla NS, and Feuvray D (1990) Intracellular pH and role of Na+/H+ exchange in cardiac sarcolemmal vesicles isolated from diabetic rats. *Am. J. Physiol.* **258,** H255-261.

Radonic A, Thulke S, Mackey IM, Landt O, Siegert W, and Nitsche A (2004) Guideline to reference gene selection for quantitative real-time PCR. *Biochem. Biophys. Res. Commun.* **313**, 856-862.

Rosen P, Du X, and Tschope D (1998) Role of oxygen derived radicals for vascular dysfunction in the diabetic heart: prevention by alphatocopherol? *Mol Cell Biochem.* **188**,103-111.

Rosenberger CM, Polland AJ, and Finlay BB (2001) Gene array technology to determine host responses to *Salmonella*. *Microbes Infect.* **3**, 1353-1360.

Rupp H, Elimban V, and Dhalla NS (1994) Modification of myosin isozymes and SR Ca^{2+} pump ATPase of the diabetic rat heart by lipid-lowering interventions. *Mol. Cell. Biochem.* **132**, 69-80.

Ryder JW, Yang J, Galuska D, Rincon J, Bjornholm M, Krook A, Lund S, Pedersen O, Wallberg-Henriksson H, Zierath JR, and Holman GD (2000) Use of a novel impermeable biotinylated photolabeling reagent to assess insulin and hypoxia-stimulated cell surface GLUT4 content in skeletal muscle from type3 diabetic patients. *Diabetes* **49**, 647-654.

Schmittgen TD, and Zakrajsek BA (2000) Effect of experimental treatment on housekeeping gene expression: validation by real-time, quantitative RT-PCR. *J. Biochem. Biophys. Methods.* **46,** 69-81.

Sowers JR, Epstein M, and Frohlich ED (2001) Diabetes, hypertension, and cardiovascular disease: an update. *Hypertension* **37**,1053-1059.

Steiner DF (1977) Insulin today. *Diabetes* **26**, 322-332.

Steiner G (2000) Lipid intervention trials in diabetes. *Diabetes Care* **23** *Suppl* **2**, B49-53.

Teshima Y, Takahashi N, Saikawa T, Hara M, Yasunaga S, Hidaka S, and Sakata T (2000) Diminished expression of sarcoplasmic reticulum Ca^{2+}-ATPase and ryanodine sensitive Ca^{2+} channel mRNA in streptozotocin-induced diabetic rat heart. *J. Mol. Cell. Cardiol.* **32**, 655-664.

Unsitupa MI, Mustonen JN, and Airaksinen KE (1990) Diabetic heart muscle disease. *Ann. Med.* **22,** 377-386.

Valle HF, Lascano EC, Negroni JA, and Crottogini AJ (2003) Absence of ischemic preconditioning protection in diabetic sheep hearts: Role of sarcolemmal KATP channel dysfunction. *Mol. Cell. Biochem.* **249**, 21-30.

Valverde AM, Lorenzo M, Navarro P, Mur C, and Benito M (2000) Okadiac acid inhibits insulin-induced glucose transport in fetal brown adipocytes in an Akt-independent and protein kinase C zeta-dependent manner. *FEBS Lett.* **472**, 153-158.

Van Holde KE, and Hill WE (1974) General physical properties of ribosomes. In: Ribosomes. *Cold Spring Harbor Laboratory, Cold Spring Harbor, New York. pp* 53-91

Vandesompele J, De Preter K, Pattyn F, Poppe B, and Van Roy N (2002) Accurate normalization of real time quantitative RT-PCR data by geometric averaging of multiple internal control genes. *Genome Biology* **3,** 0034.1-0034.11

Vetter R, Rehfeld U, Reissfelder C, Weiss W, Wagner KD, Gunther J, Hammes A, Tschope C, Dillmann W, and Paul M (2002) Transgenic overexpresiion of the sarcoplasmic reticulum Ca^{2+} ATPase improves reticular Ca^{2+} handling in normal and diabetic rat hearts. *FASEB J.* **10**. 1657-1659.

Virkamaki A, Ueki K, and Kahn CR (1999) Protein-protein interaction in insulin signalling and the molecular mechanisms of insulin resistance. *J. Clin. Invest.* **103**, 931-943.

Wang EM, Liu C, and Dziarsk R (2000) Chemokines are the main proinflammatory mediaties in human monocytes activated by *Staphylococcus aureus*, peptidoglycery and endotoxin. *J. Biol. Chem.* **275**, 20260-20267

Weimer B, Xie Y, Chon L, and Catler A (2004) Gene expression arrays in food. In: Barredo JL (ed) Microbial products and biotransformation. Humana Press. Totowa. N.J. pp333-343.

White MF, Kahn CR (1994) The insulin signalling system. *J. Biol. Chem.* **269**, 1-4.

Wood H, Reischl U, and Peeling RW (2002) Rapid detection and quantification of *Chlamydia trachomatis* in clinical specimens by LightCycler PCR. In: Reischl U, Wittner C, Cockerill F, editors. Rapid cycle real time PCR: methods and applications, microbiology and food analysis. pp115-132.

Xie T (2003) Determining the influence of extracellular proteinase from *Brevibacterium linens* on the metabolism of *Lactococcus Lactis* spp. Lactis using functional genomics. Ph. D dissertation. Utah State University. Logan.

Yechoor VK, Patti ME, Saccone R, and Kahn RC (2002) Coordinated patterns of gene expression for substrate and energy metabolism in skeletal muscle of diabetic mice. *Proc. Nat. Acat. Sci. USA.* **99**,10587-10592.

Young M.E, McNulty P, and Taegtmeyer H (2002) Adaptation and maladaptation of the heart in diabetes: Part II. *Circulation*, **105**, 1861-1870.

Zhong H, and Simons JW (1999) Direct comparison of GAPDH, beta-actin, cyclophilin, and 28S rRNA as internal standards for quantifying RNA levels under hypoxia. *Biochem. Biophys. Res. Commun.* **259**, 523-526.

Ziegelhoffer-Mihalovicova B, Waczulikova I, Sikurova L, Styk J, Carsky J, and Ziegelhoffer A (2003) Remodelling of the sarcolemma in diabetic rat hearts: The role of membrane fluidity. *Mol. Cell. Biochem.* **249**, 175-182.